

DOKUZ EYLÜL UNIVERSITY
GRADUATE SCHOOL OF NATURAL AND APPLIED SCIENCES

**PRODUCTION OF MATERIALS WITH
DIELECTRIC PROPERTIES FOR
NEUROSTIMULATOR**



by
Ozan YILMAZ

June, 2016
İZMİR

PRODUCTION OF MATERIALS WITH DIELECTRIC PROPERTIES FOR NEUROSTIMULATOR

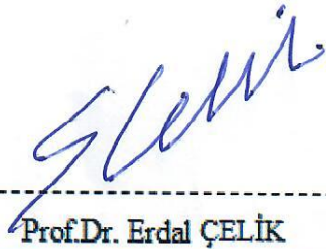
**A Thesis Submitted to the
Graduate School of Natural and Applied Sciences of Dokuz Eylül University
In Partial Fulfillment of the Requirements for the Degree of Master of
Science in Department of Nanoscience and Nanoengineering**

**by
Ozan YILMAZ**

**June, 2016
İZMİR**

M.Sc. THESIS EXAMINATION RESULT FORM

We have read the thesis entitled “**PRODUCTION OF MATERIALS WITH DIELECTRIC PROPERTIES FOR NEUROSTIMULATOR**” completed by **OZAN YILMAZ** under supervision of **PROF.DR. ERDAL ÇELİK** and we certify that in our opinion it is fully adequate, in scope and in quality, as a thesis for the degree of Master of Science.



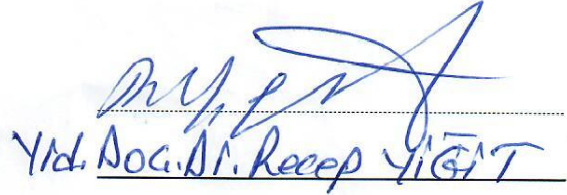
Prof.Dr. Erdal ÇELİK

Supervisor



Doc.Dr. Ömer NERUER

(Jury Member)



Yrd. Doç. Dr. Recep YIGİT

(Jury Member)



Prof. Dr. Ayşe OKUR

Director

Graduate School of Natural and Applied Sciences

ACKNOWLEDGMENTS

I would like to express my deep sense of gratitude to my advisor Prof.Dr. Erdal ÇELİK for his constructive ideas, help, constant support, guidance and contributions. I would also like to thank my committee members for reviewing my work and offering valuable suggestions and sharing their visions about the content of my thesis. I would like to thank Serdar YILDIRIM, Metin YURDDAŞKAL, Tuncay DİKİCİ and for their invaluable assistance and kind friendship.

This research was funded by Tübitak 1003 Researching Project with the name “Small Size Neurostimulator and External Transfer Module Designing and Placing Intravascular Into The Body Project” and project number 113S080. Due to fact that I would like to thank Tübitak and DEU-EMUM for their economical and infrastructural supports.

A special thank goes to my dear family Gül YILMAZ and Mustafa YILMAZ for their concern, confidence and support. In addition, special thanks goes to my dear friends Serdar GÜLTEKİN and Gökay ŞERİF. The successful completion of this study would not have been possible without their constant love and encouragement.

Ozan Yılmaz

PRODUCTION OF MATERIALS WITH DIELECTRIC PROPERTIES FOR NEUROSTIMULATOR

ABSTRACT

Besides the fact that the foundations of neurophysiology and electrophysiology dating back to a hundred years ago, neurostimulation usage in illness or symptomatic cures began provoking thoughts after the second world war. As known, the fact that nerve cells carrying information from one side of the nerve system to the other is an electrical phenomenon. 'Action potential' which occurs and transmitted from in nerve cells membrane via ion channel play the leading role in this phenomenon. Any change in action potential creates a domino effect making nerve cells transmit the change from one to the other via synapsis. Nerve cells prepare itself to answer any forthcoming call by keeping ion channels active and normalizing action potential. Neurostimulators, which works when such a normalization system is out of order are becoming more and more important.

It is said that there have been successful attempts around the world in neurostimulator way of cures with a 70% success ratio compared with chemical medication. Therefore, the design and production phase of neurostimulators are also in key role when it comes to performance. The key factor when identifying action potential created by neurostimulator is the electrical capacity and dielectric constant of related material.

The main purpose of this project is to choose necessary material to maximize the performance of neurostimulator. In addition, the other purpose is, by using sol gel production method to cover semiconductive wafers with aluminum oxide, titanium oxide, polymethyl methacrylate and polyvinyl alcohol and to understand structural, microstructural, electrical and morphological characterization of those materials.

Keywords: Sol gel, neurostimulator, dielectric constant semi conductive

NÖROSTİMÜLATÖR İÇİN DİELEKTRİK ÖZELLİKLERE SAHİP MALZEME ÜRETİMİ

ÖZ

Nörofizyoloji ve elektrofizyolojinin temellerinin atılması bir yüzyıl geriye gidebilmekle birlikte, nöromodülasyon ile hastalık ya da semptomik tedaviler ikinci dünya savaşından sonra merak uyandırmaya başlamıştır. Bilindiği üzere sinir hücrelerinin, sinir sistemimizin bir tarafından diğer tarafına bilgi taşınması “elektriksel” bir fenomendir. Sinir hücresi membranında iyon kanalları vasıtasıyla oluşan ve iletilen “aksiyon potansiyeli” bu elektriksel fenomenin oluşumunda temel rol oynar. Aksiyon potansiyelindeki değişiklik, domino taşı etkisiyle sinir hücresinden, bir diğer sinir hücresine “sinaplar” yoluyla akatarılır. Sinir hücresi, iyon kanalları aktif olarak çalıştırılarak, aksiyon potansiyelini hızla normalize ederek bir sonraki uyarıya kendini hazır eder. İşte vücutta bu normalizasyon sisteminin işlemediği durumlara çözüm olarak üretilen nöromodulatorler son dönemde önemini iyice artırmıştır.

Dünyada nöromodulatorler ile yapılan tedavilerde, kimyasal ilaçlara göre daha iyi sonuç alındığı, yüzde yetmişlere varan tedavi başarı oranına kadar ulaşıldığı belirtilmiştir. Dolayısıyla üretilen nöromodulatorlerin tasarım ve üretimi de performansında etkileyici rol oynamaktadır. Nöromodulatorlerin yaratacağı aksiyon potansiyelini belirleyen en önemli faktör ise elektrik kapasitedir ve bunun için seçilecek malzemenin dielektrik katsayısı rol oynamaktadır.

Bu çalışma, üretilecek olan nöromodulatorün performansını en üst seviye de tutmak için kullanılacak malzelerin seçimi üzerinedir. Sol-jel yöntemi ile alüminyum oksit, titanyum oksit, polimetilmetakrilat ve polivinil alkolü yarıiletken waferlar üzerine kaplanmıştır ve bu malzemelerin karakterizasyonları gerçekleştirilmiştir.

Anahtar Kelimeler: Sol-gel, nörostimulator, dielektrik katsayısı, yarı iletken

CONTENTS

	Page
THESIS EXAMINATION RESULT FORM	ii
ACKNOWLEDGEMENTS	iii
ABSTRACT	iv
ÖZ	v
LIST OF FIGURES	x
LIST OF TABLES	xiii
CHAPTER ONE- INTRODUCTION.....	1
1.1 General.....	1
1.2 Organization of The Thesis	5
CHAPTER TWO- THEORETICAL BACKGROUND.....	7
2.1 Neurostimulation	7
2.1.1 Principle of Neurostimulation.....	7
2.1.2 Usage Area of Neurostimulation	8
2.1.3 Electrical Dimension of Neurostimulators and Correlation Between Dielectric Constant	10
2.1.4 Material Selection Based On Electrical Dimension of Neurostimulators and Dielectric Constant.....	11
2.1.5 Neurostimulator Design And Produce Systems	12
2.2 Sol-Gel Method	14
2.2.1 Steps of Sol-Gel Method	15
2.2.1.1 Hydrolysis	18
2.2.1.2 Condensation.....	19
2.2.1.3 Polymerisation	20

2.2.1.4 Gelation.....	22
2.2.1.5 Aging.....	23
2.2.1.6 Drying	24
2.2.1.7 Sintering.....	27
2.3 Spin Coating	27
2.3.1 Spin Coating General Theory	27
2.3.2 Description of Spin Coating Process	28
2.3.3 Spin Coating Thickness Equation.....	29
CHAPTER THREE- EXPERIMENTAL.....	32
3.1 Purpose of Thesis	32
3.2 Materials.....	33
3.2.1 Substrate Preparation.....	33
3.2.1.1 Silicon Single Crystal Growing.....	33
3.2.1.2 Silicon Ingot Slicing Process	34
3.2.1.3 Lapping&Polishing Process.....	35
3.2.1.4 Silicon Ingot Cutting Process.....	36
3.2.2 Solution Preparation	39
3.2.2.1.Preparing of Metal Oxide Groups Samples	39
3.2.2.2 Preparing of Polymer Groups Samples.....	39
3.2.3 Spin Coating	40
3.2.3.1 Spin Coating Process for Metal Oxide Groups.....	40
3.2.3.2 Spin Coating Process for Polymer Groups	40
3.2.4 Heat Treatment	42
3.3 Characterization.....	45

3.3.1 Solution Characterization	45
3.3.1.1 Ph Measurement.....	45
3.3.1.2 Turbidity Measurement.....	46
3.3.1.3 Contact Angle	46
3.3.1.4 Fourier Transform Infrared Spectropy.....	46
3.3.2 Materials Characterization.....	47
3.3.2.1 Differential Thermal Analysis-Thermal Gravimetric Analysis (DTA-TGA)	47
3.3.2.2 X-Ray Diffractometer	48
3.3.2.3 Scanning Electron Microscopy (SEM)	49
3.3.2.4 Dielectric Measurement.....	50
CHAPTER FOUR- RESULT AND DISCUSSION.....	52
4.1 Solution Results.....	52
4.1.1 PH Results	52
4.1.2 Turbitidy Results	52
4.1.3 Wettability Results.....	53
4.1.3.1 Determination of The Contact Angle of Metal Oxide Sample	53
4.1.3.1 Determination of The Contact Angle of Polymer Sample.....	54
4.2 Materials Process Optimization.....	55
4.2.1 Differential Thermal Analysis-Thermal Gravimetric Analysis (DTA-TGA)	55
4.2.2 Fourier Transform Infrared Spectropy (FTIR)	57
4.2.2.1 FT-IR Analysis for Metal Oxide Group.....	58
4.2.2.1 FT-IR Analysis for Polymer Group	61
4.3 Phase Analysis.....	62

4.3.1 Phase Analysis for Metaloxide Samples.....	63
4.3.2 Phase Analysis for Poylmer Samples	64
4.4 Microstructure Analysis / Energy Dispersive X-ray Spectroscopy (EDS)	65
4.4.1 Microstructure Properties of Metal Oxide Groups	66
4.4.2 Microstructure Properties of Polymer Groups.....	68
4.5 Dielectric Properties	69
4.5.1 Dielectric Properties of Metal Oxide Groups	69
4.5.2 Dielectric Properties of Polymer Groups.....	70
CHAPTER FIVE- CONCLUSION AND FUTURE PLANS.....	73
5.1 General Results.....	73
5.2 Future Plans	74
REFERENCES.....	75

LIST OF FIGURES

	Page
Figure 2.1 Part of sending aerial for neurostimulator design.....	12
Figure 2.2 Part of receiving aerial for neurostimulator design	12
Figure 2.3 Neurostimulator and lead systems used for spinal cord stimulation to treat chronic pain. The Itrel 3 and the Synergy are neurostimulators. The Synergy EZ is a patient programmer. Including percutaneous leads (top) and surgical leads (bottom).	13
Figure 2.4 Hydrolysis process	18
Figure 2.5 Condensation of olation and oxalation..	19
Figure 2.6 (a) The structure of acid catalyst mechanism (b) The structure of basic catalyst mechanism.....	20
Figure 2.7 Polymerization.....	21
Figure 2.8 Gelation.....	23
Figure 2.9 Four distinct stages to spin coating.....	28
Figure 2.10 Drop casting slowly without rotation is a good way to provide highly ordered films at the nanoscale but at the expense of uniformity across the substrate.....	29
Figure 3.1 PVA Tepla Czochralski single crystal ingot and wafer.....	34
Figure 3.2 STX-1202 slicing device and slicing process.....	35
Figure 3.3 Slide silicon ingot lapping process	36
Figure 3.4 Lapping and polishing process parameters.....	36
Figure 3.5 1x1 cm and 2x2 cm samples for cutting process	37
Figure 3.6 (a) 2x2 cm and (b) 1x1 cm cutting wafers.....	37
Figure 3.7 SEM results for pure Si.....	37
Figure 3.8 EDS results for pure Si	38
Figure 3.9 XRD pattern for pure Si.....	38
Figure 3.10 Flowchart for prepatation of metal oxide samples	39
Figure 3.11 Spin rate/time schedule for metal oxide groups	40
Figure 3.12 Spin rate/time schedule for PVA	41
Figure 3.13 Spin rate/time schedule for PMMA.....	41

Figure 3.14 Protherm (metal oxide group) and Nüve MF120 oven (polymer) for heating processes.....	42
Figure 3.15 Heat treatment for TiO ₂ of metal oxide group	43
Figure 3.16 Heat treatment for Al ₂ O ₃ of metal oxide group	43
Figure 3.17 Dehydration regimes for PVA	44
Figure 3.18 Dehydration regimes for PMMA.....	44
Figure 3.19 HANNA HI83141 pH meter.....	45
Figure 3.20 VELP TB1 turbidimetry	46
Figure 3.21 Thermo Scientific Nicolet iS10	47
Figure 3.22 PerkinElmer STA 6000 Model Differential Thermal Analysis-Thermal Gravimetry	48
Figure 3.23 X-Ray Diffraction.....	49
Figure 3.24 Novocontrol Alpha-N High Resolution Dielectric Analyzer	50
Figure 3.25 Dielectric illustration	51
Figure 4.1 Al ₂ O ₃ solution contact angle.....	54
Figure 4.2 TiO ₂ solution contact angle	54
Figure 4.3 PVA solution contact angle	55
Figure 4.4 PMMA solution contact angle	55
Figure 4.5 DTA-TG result for Al ₂ O ₃ precursor solution.....	56
Figure 4.6 DTA-TG result for TiO ₂ precursor solution	57
Figure 4.7 FT-IR result Al ₂ O ₃ metal oxide precursor	58
Figure 4.8 FT-IR result for calcined Al ₂ O ₃	59
Figure 4.9 TiO ₂ precursor metal oxide solution	60
Figure 4.10 Calcined TiO ₂	60
Figure 4.11 PVA FTIR analysis in air atmosphere	61
Figure 4.12 PMMA FTIR analysis in air atmosphere.....	62
Figure 4.13 XRD pattern of Al ₂ O ₃ thin film	63
Figure 4.14 XRD pattern of TiO ₂ thin film	64
Figure 4.15 XRD pattern PMMA thin film.....	64
Figure 4.16 XRD pattern of PVA thin film	65
Figure 4.17 EDS result for Al ₂ O ₃ thin film.....	66
Figure 4.18 EDS result for TiO ₂ thin film.....	66

Figure 4.19 SEM result with depicted 1000x (a) and depicted 5000x (b) for TiO ₂ ...	67
Figure 4.20 SEM result with depicted 1000x (a) and depicted 5000x (b) for Al ₂ O ₃ .	67
Figure 4.21 a) PVA 500x, b) PVA 5000x; c) PMMA 500x, d) PMMA 5000x.....	68
Figure 4.22 Permittivity of Al ₂ O ₃ thin film.....	69
Figure 4.23 Permittivity of TiO ₂ thin film	70
Figure 4.24 Permittivity of PVA.....	71
Figure 4.25 Permittivity of PMMA.....	72
Figure 4.26 Design of neurostimulator system	72



LIST OF TABLES

	Page
Table 2.1 Target areas in neurostimulation.....	9
Table 2.2 The best designing parameters for neurostimulators	10
Table 3.1 Silicon single crystalline	33
Table 3.2 The numerical result of Si single crystal.....	34



CHAPTER ONE

INTRODUCTION

1.1 General

Neurostimulators; in the context of this thesis were used as electronic systems that provide neurotic activation and inhibition inside the body through a signal which was created between necessary frequency gaps, via an energy system that may be inner or outer.

Neurostimulators, that are implanted inside the body, may be in shape of a battery provide adequate sustainable energy for 5-10 years or may be in a form of a battery that can be charged outside. These well-known systems have well-known technologies.

In the context of this thesis, the emphasis was given on design and manufacture process of implantable neurostimulator systems, substructure material production for configuring electricity, determining characteristic features and estimation of electric performance. Dielectric constant that was used to determine electric features and performance related frequency gap effects were researched. Thus, how to enhance the performance of long-known neurostimulators via various materials usage was understood.

In order to select a standard neurostimulator to implant inside the body, the emphasis was given to a silicon (SiO_2) based material selection which is semi-conductive and applicable coating selection so as to create an electronic.

In addition to these coatings, components to modulate on device are a receiver coil, rectifier diode, capacitor and a constant current field electric transistor for stimulation. Having stimulation electrode coated with palladium, gold or platinum, that are compatible with the human body and having those in monopole form is of great importance for human body. Stimulation parameters, on the other side, may be placed

as an adjustable system with RF power transmit on unite. On the top of the factors that determine neuromodulator performance that host electrical and component system comes applied signal the semi-conductive plate that host components to carry the signal and the thin film coating that the plate has.

In the context of this thesis coating materials, coating those materials on silicon via sol-gel method and performances of achieved products were researched and compared. Semi-conductive the silicon material to coat and materials used for were chosen among metal oxide and polymer group. The method and analyses of the thesis were determined in the light of thesis made around the world on this subject among the reasons why the analyses conducted on this issue were made in the light of those thesis, is that materials needed to produce neurostimulators belong to metal oxide and polymer groups.

By selecting two different materials amount two different groups, their usage areas, both inside and outside their groups, dielectric features, processes were compared. Titanium oxide and aluminium oxide from metal oxide group, polyvinyl alcohol and polymethylmethacrylate from polymer group were chosen for this analyses. Single crystal ingot which was created with PVA Tepla Czochralski single crystal growing device, silicon wafer on sol-gel and the thin film via spin coating method (described by Chapter 2) were constituted. Comparing literature values with thin film performances and characterisation, optimisation and electronic appropriateness of the structure and its performance were identified. The performance of coatings and component addition on them to make them ready for neurostimulator usage were targeted. As a result of those analyses, characteristic features and optimize values will show that the materials are useable for neurostimulator production and dielectric measurement value show the performance.

Lots of examples are available in the world literature about this system. In the literature part of this thesis, firstly neurostimulator structure and then creating substructure of it were benefitted from. After that the sol-gel method, which is used for creating those substructure materials, immediately after metal oxide and polymer

based materials that were produced to use for coating, material characterization dielectric measurement was utilised.

Rise (2000) who is among those, in his thesis on neurostimulators, demonstrated examples on simple working principles of neurostimulators, their usage in biophysics field, the necessary electronic configuration of the device and other implantable samples. At the heart of this thesis, performance parameters of the device which is responsible for activation and passivation of nerve cells were taken a neurostimulators has to have as:

‘Reduced to its simplest form, a neurostimulator consists of a power supply, i.e., a battery, a pair of electrodes in contact with the tissue, extension wires to connect the electrodes to the battery, and a switch that enables the power to be intermittently connected to the electrodes.... Conventionally, there are two types of electrode configurations, referred to as monopole and bipolar stimulation. Of course, for current to flow it is necessary that there be two electrodes, a positive anode and a negative cathode. Monopole stimulation, then, refers to an electrode configuration that includes an electrode of a relatively small surface area located near or in the nervous tissue to be stimulated. This electrode is typically the negative electrode or cathode for reasons described later in this work. The positive electrode has a larger surface area and is located remote to the stimulation target’ Rise (2000).

Another literature research about neurostimulator is that Parpura et al. (2012) have published an article entitled ‘‘Neuromodulation: selected approaches and challenges’’. In this review can be summarized that selected approaches and challenges in neuromodulation and then the use of water-dispersible carbon nanotubes has been proven effective in the modulation of neurite outgrowth in culture and in aiding regeneration after spinal cord injury in vivo. Having this analyses as a guide, one of the coating material was chosen as polymer group. Neurologically it was envisioned that polymer coating would suit well when working principles of brain, nerve and muscle taken into account during the integration process of electronic circuit in order to make sure the circuit is working well with the body. ‘‘Toxicity is less likely to be

of such grave concern when the carbon nanotubes/nanofibers are attached to electrodes and are coated with a conducting polymer of proven safety in vivo, such as polypyrrole or polyimide.’’ Parpura et al. (2012). Thus, in this context of this thesis, PVA and PMMA which were chosen from polymer group, and electronic performance of coating material were studied.

In the other working group, again one of the most studied group, the metal oxide group, was studied. In addition to semi-conductive plate which is necessary for neurostimulator, it is possible to add components on modulation electrically by thin film structure. In the literature, among thin film coating techniques, the sol gel method constitutes lots of various techniques in terms both polymer and metal-oxide group.

Guglielmi (1997) has studied about ‘‘Sol-Gel Coatings on Metals’’. In this study sol-gel derived films can be deposited on metals to improve their resistance to oxidation and corrosion or to modify their surface properties.

However, usual applications are limited by problems intrinsic to sol-gel processing or specific of coating/metal systems. An important aspect of the application of the sol-gel method for coating metallic objects is also the deposition technique. Result of this researching for sol gel is that it gives general processing about sol gel and also related problems with sol gel.

Other important studies on thin film manufacture through sol-gel techniques are, Kazemi & Mohammadizadeh (2012) have published ‘‘Simultaneous improvement of photocatalytic and super hydrophilicity properties of nano TiO₂ thin films’’ and Ruys & Mai (1999) have entitled ‘‘The nanoparticle-coating process: a potential sol–gel route to homogeneous nanocomposites’’ and also especially important study is that Brinker & Scherer (1990) have published their books ‘‘ Sol-Gel Science’’ and also Innocenzi, Zub & Kessler (2008) have edited ‘‘Sol-Gel Methods for Material Processing’’. Especially in these studies are focused sol-gel method and its processing system.

1.2 Organization of The Thesis

The purpose of this thesis is to produce the semi conductive silicon wafer which is necessary for designing and producing the device that periodically stimulate the muscles inside the body by stimulating applied frequencies on the device and adjusting necessary electronic components called neurostimulator on it. Besides, thin film coating and determining characteristically features of these coating was also aimed. Hence, evaluating electrical performance of produced coating material and comparing experiment groups with each other aimed as well. So as to complete this study, it was planned to produce the material by using sol-gel and spin coating techniques and then to compare the two groups, that was determined as polymer and metal-oxide, according to their dielectric result. According to these estimations, designing and producing parameters of neurostimulator will be determined.

Accordingly, in the first part of thesis organization, emphasis was given on neurostimulator systems, context of the thesis and consecutive analysis, experiments and results.

In the second part literature support was given for creating neurostimulator structure, extensive research on these stimulators production techniques used in creating structure like sol-gel and spin coating.

In Chapter Three, emphasis was given on semi-conductive plate manufacture according to theoretical sub-structure, the experiments conducted on these semi-conductive plates for creating thin film (Al_2O_3 , TiO_2 metal oxide group and PVA, PMMA polymer group) by sol-gel and spin coating techniques devices we used and production prescription, heat treatments, characterization and optimization.

In Chapter Four, emphasis was given the results obtained from empirical studies and interpreting them. The semi-conductive silicon that we need for neurostimulator production and appropriateness of coating material for production were examined and

then by dielectrical estimation, performance results were obtained and their levels of applicability were compared.

In chapter five, propositions, studies and plans that this thesis may enlighten were mentioned.



CHAPTER TWO

THEORETICAL BACKGROUND

2.1 Neurostimulation

The recuperation of illnesses stemming from nerve transmission as they cannot renew themselves, is harder than other illnesses of organs. Along with not having a full curative effect, chemical triggering of nerve cells which work with electrical stimulation, may cause to deterioration right after you stop medication. Replacing chemical medication with neurostimulator recently has been more curative and has been increasing the chance of recuperation.

2.1.1 Principle of Neurostimulation

Transmitting information from one side of the nerve system to the other side is a system which leans on electrical axis and action potential which is created thanks to the nerve cell membrane ions create the roots of this electrical event. Any change in action potential is transmitted through nerve cells via synapsis. As a result, nerve cells use ion channels, make them work actively, normalize action potential and get ready for the next phase.

If electrode is placed near nerve cells and a special outer tension is applied, the tension in nerve cell membrane activates sensitive ion channels and changes action potential of nerve cell. This change may cause a nerve activation through changing action potential of other nerve cells via synapsis. The opposite of this process is also right: another special tension on electrodes may block created action potential transmission from one cell to the other. This is called nerve inhibition.

The process of placing electrodes in, on the surface or near the anatomical elements which constitutes central or environmental nerve systems and creating activation or inhibition via a special tension from those electrodes is called neurostimulator. Along

with achieved neurostimulator effect the probability of curing the leading nerve system maladies like Parkinson's or spinal cord injuries and secondary nerve system malfunctions like migraine or neuropathic may become possible (Peckham et al., 2005).

2.1.2 Usage Area of Neurostimulation

While the roots of neurophysiology and electrophysiology dates back to a hundred years ago, symptomatic or illness remedies started provoking thoughts right after the Second World War. The first successful application in this field has been the heart battery device called "peacemaker". Deep brain stimulators like the ones which are placed on spinal system to cure pain and Parkinson's disease has also been other successful applications.

The material choice of production of neurostimulators, which constitutes the basis of this research, depends according to usage area. In addition to this, according to implantation processes, to create a specific nerve trigger, there has been frequency gaps. These frequencies have to be designed according to implant area and neurostimulation process should be conducted.

A typical implantable neurostimulator device consists of an electrode-cable system inside related nerve system and battery-electronic circuit tanks. Electrodes are implanted with a surgical operation.

The tank part is put inside a pocket under the skin. (No part is left above the skin). For this reason, there may sometimes be big and risky operations around brain, face cavities, neck, chest cavity, abdomen pelvic and pubic.

Some well-known target areas and medical justification in neurostimulator is shown in table (Table 2.1). New nerve stimulation and remedies are added every year. There has also been some influx in medical usage. The neurostimulator market in USA has raised to 2 billion \$ from 500 million \$ between 2005-2010. In USA market, these

devices are traded around 15.000-30.000\$ (except hospital expenditures) (Panescu, 2008).

Table 2.1 Target areas in neurostimulation (Panescu, 2008).

PLACE	INDICATION
Spinal Cord	Pain Relief
Brain Basal Ganglia's	Parkinson's and similar illnesses
Vagal Nerve	Epilepsy, Migraine, Depression
Phrenic Nerve	Respiration Paralysis
Occipital Nerve	Headache, Migraine
Sphenopalatine Ganglia	Paralysis, Vasospasm, Migraine
Otic Ganglia	Migraine
Hypoglossal Nerve	Snoring, Sleep apnea syndrome
Gastric Nerves	Morbid obesity, lazy stomach
Sacral Nerves	Urinary/Gaita incontinence
Pudental Nerve	Urinary/Gaita incontinence
Cochlear Nerve	Deafness
Arm/Leg Nerves	Paralysis related inactivity

Implantable neurostimulators has developed technologically during the last 10-15 years. The main reason for this is to reduce surgical operations during implantation and risks to comfort patients.

Another reason for this is that the number of neurostimulator usage in medical operations and its curative efficiency in illnesses are rising steadily and swiftly. Since high-tech implantable neurostimulators are operated effectively with outer RF energy transfer systems these days, they reached tinier levels (Panescu, 2008).

2.1.3 Electrical Dimension of Neurostimulators and Correlation Between Dielectric Constant

When choosing parameters, frequencies that let nerves transmit electrical signal must be chosen. The stimulating parameters must be chosen accordingly with the situation and anatomy of the patient that will be stimulated. To make his reality, neurostimulators should be designed adjustable. In other words, a design which is programmable from outside should be created.

While choosing design criteria, using MICS (Medical Implant Communication Service) frequencies is of primary importance. Making the communication between remote control and stimulator device with an implanted tool on human body necessitates it to be on a harmless radiation level not to harm the patient. In this respect, while choosing communication components in designing phase, frequencies that suits MICS frequency standards and materials that are harmless must be chosen. Neurostimulator designing parameters are given in Table 2.2 with all requirements.

Table 2.2 The best designing parameters for neurostimulators (Hannan et al., 2014; Olivo, 2011; Tucker, 2011; Yuan, 2011)

Signal Type	Frequency	Pulse Type	Stimulate	Current (mA)	Voltage (V)	Power (mW)
Signals to be transmitted to the nerves	0-200 Hz	Square	Pulse and Width	0.1 - 5	1 - 5	0.1 - 25

Index given in Table 2.1 (Hannan et al.,2014; Olivo, 2011; Tucker, 2011; Yuan, 2011) covers the necessary features of control part and stimulating part of neurostimulator. Stimulating frequency is the frequency stimulating signal which is transmitted to electrodes. Pulse type means the pulse type that is supposed to be produced by remote control.

There may be several different stimulation choices. Because the least expensive is the PWM, it is added to the bests table. Current constant, tendency constant and the amount of power, which are supposed to be transmitted via electrodes to tissue, were also given in the table. 1-20 Hz signal is needed to make nerves activated through human tissue. 20-200 Hz frequency indexes are used to make nerves de-activated.

These parameters must be kept, changing from person to person. That's why the designed neurostimulators must be in such a condition that it can be controlled outside with a remote control whenever it is wanted.

The characteristic features of human tissue are very important. Generally, the impedance of human tissue per millimetre changes between 600-1200 Ω (Hannan et al., 2014).

2.1.4 Material Selection Based On Electrical Dimension of Neurostimulators and Dielectric Constant

When an outer electrical field is applied to the material, and if the material saves energy after that, it is classified as "dielectric". Dielectric constant, shows how much energy is saved in outer electrical field and how much energy is lost inside the material when it is under the effect of a field. Dielectric constant of the material is an amount that reduces the electrostatic power between two electrical charge (Göver, 1996).

Dielectric materials don't transmit electric. However, they are affected by applied electrical field. Under the effect of electrical field, electrons and atoms switch places. Because of this, electrical load centres change and electrical polarization occurs.

The occurred electrical dipolar, provides the electrical charge accumulation on dielectric material surface. That's why they are used in capacitor production. The reason why they are used as dielectric is that they block charge transfer in electric circuit (Erdogan, 1997).

2.1.5 Neurostimulator Design and Produce Systems

The electrical configuration that standard neurostimulators must have are; oscillator, controller, modular, empowered and transmitter circuit system (Figure 2.1) and electrode, capacitor, filter, DC battery and demodulator system that make neurotic stimulation to the patient via receiver circuit system.

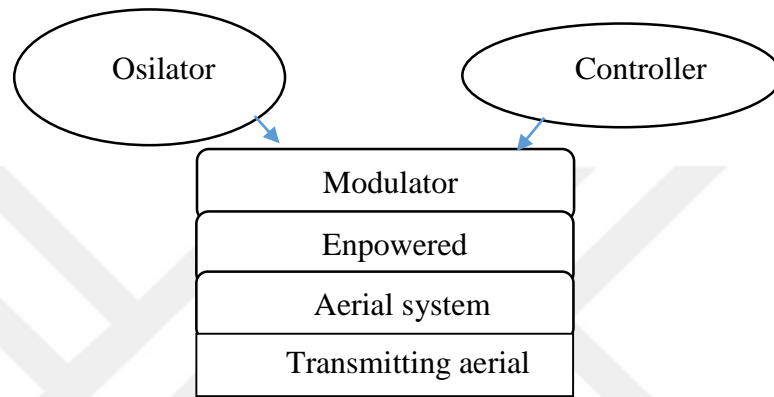


Figure 2.1 Part of sending aerial for neurostimulator design

RF waves applied from outside, designed in order to stimulate nerves when it is implanted inside the body from transmitter circuit to receiver circuit. In the systems with battery, received signal is fortified with noise in fortifier, before demodulation. By filtering and demodulating, strike figure that is produced in transmitter is maintained. In systems that are powered through air, the received signal from the antenna directly transformed into DC tension via rectifier and is filled into capacitor.

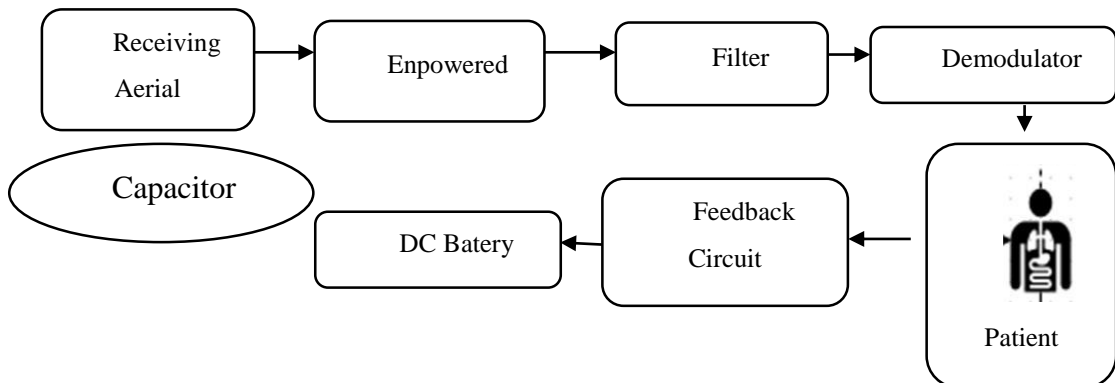


Figure 2.2 Part of receiving aerial for neurostimulator design

Parallel, signal is strengthened with obtained power and is prepared for the next phases. After filtering and demodulation, process is conducted like the systems with battery (Figure 2.2) (Hannan et al., 2014).

While PWD is transmitted through electrodes to tissue electrode driving circuit must be designed to retreat the load that is transmitted to the body, in order not to harm the tissue. Electrode must be produced from harmless materials like platin, titanium.

The material that we use an electrical configuration was chosen as silicon single crystal, a semi-conductive material. Si wafers are preferred because of their features such as electrical transmission during device production, load storage, load transfer. Coating applied on silicon wafer prepares the right environment for neurostimulator production. Sol-gel method is the one used most in creating that coating (Yuan, 2011).

Ultimately, the materials used in electronic design of neurostimulator are prepared and the design is conducted accordingly with usage area and working principle. Figure 2.3 is a picture of the group of neurostimulator products used to treat chronic pain and includes pictures of the different styles of surgical leads available and the leads are flat and paddle shaped, with four or more electrodes located on the spinal cord side of the paddle (Rise, 2000).



Figure 2.3 Neurostimulator and lead systems used for spinal cord stimulation to treat chronic pain. The Irel 3 and the Synergy are neurostimulators. The Synergy EZ is a patient programmer. Including percutaneous leads (top) and surgical leads (bottom) (Rise, 2000).

2.2 Sol-Gel Method

In the context of this research, polymer and based two materials were chosen from the group that we were planning to coat our semi-conductive wafers with. In order to produce these materials with sol-gel method, the sol-gel method must be understood profoundly first.

The sol-gel method is a wet chemical technique that uses metal alkoxides for the synthesis of ceramics through a series of chemical processes including hydrolysis, gelation, drying, and thermal treatment (Metroke, 2001; Livage, Beteille, Roux et al., 1998). The metal alkoxides are subjected to the hydrolysis. A mixture of water, alcohol and hydrochloric acid are added into the precursor metal alkoxides mixture by drop wise. The hydrolysis reaction of metal alkoxides with water in the presence of HCl catalyst takes place that produce hydroxide of precursors (Znaidi, 2010; Livage, Beteille, Roux et al., 1998).

A sol is defined as a colloidal of solid particles suspended in liquid. A gel, on the other hand, is a composite substance consisting of continuous solid skeletal structure, which results from the gelation of the sol. The gel obtained is mixed with appropriate amount of flux if needed and grinded to form fine powder. The mixture powder is then subjected to thermal treatment at various temperatures according to need of the final phosphor product. The sol-gel method owes following overcomes above the solid state method and have been using extensively in phosphor research. (Hamadianian, Reisi-Vanani & Majedi, 2010; Mohammadi & Fray, 2011; Pierre, 1998; Wright, 2001),

1. Higher homogeneity of the chemical composition in the material product.
2. High uniformity of doping ions distribution, no local concentration quenching will occur because of impurity clustering.
3. Processing temperature can be very low. This allows the doping of fragile organic and biological molecules into porous inorganic materials and fabrication of organic-inorganic hybrid materials.

4. The controlled microstructure (pores and particles distributions). High density materials can be produced at high annealing temperature.
5. By spinning or dipping method, thin films and multi layered coating can be obtained.
6. Fine, uniform particles can be obtained that reduced the crystal destruction by milling and crushing as in solid state methods.

However, some disadvantages of this method also exist: (Pierre, 1998; Wright, 2001)

1. For transparent samples, the annealing process should be slow and deliberate, otherwise, cracks and striations will appear in the samples.
2. To remove organic groups completely, high temperature heating above 1000°C is required, that may produce undesirable side products.
3. It is well suited for micro-scale production, but very expensive and unsuitable for mass production.

2.2.1 Steps of Sol-Gel Method

Because the sol-gel method can occur in room temperature and can be obtained in different forms, sizes and formats, its usage is increasing in various scientific and engineering industries (Aurobind, Amirthalingam & Gomathi, 2006; Li, Fries & Malik, 2004; Livage, Beteille, Roux, et al., 1998). The term sol-gel defines the processes of gels which sol or colloidal suspensions are produced from.

As you can understand from the name 'sol-gel', it involves the process that we use to produce inorganic matrix by colloidal suspension, the gelling of sol to create a group gel and dry gel transformation after drying process (Aurobind, Amirthalingam & Gomathi, 2006).

Generally, the sol-gel method involves hydrolysis and condensation of a metal-organic pre-starter like tetra n-butyl titanate in a catalyst or non-catalyst environment,

inside a proper solvent like ethanol (Metroke, 2001; Mackenzie & Bescher, 2007). Synthesising of rigid materials by sol-gel method generally involves wet chemical reactions. However, the chemistry of sol-gel, depends on the transformation of molecular pre-starters in oxide bond by hydrolysis and condensation. Alkoxide groups in alcohol-water solution, leaves the environment gradually with hydrolysis via acidic, basic catalyst and replace itself with hydroxyl group that create M-O-M bonds. Gelling occurs, in order to create a bond that cover whole solution volume, with increasing polymer bonds coming together (polymerisation). In this gelling point, both viscosity and elasticity module gradually increase. Then, gel may be vaporised to create xerogel (Aurobind, Amirthalingam, Gomathi, 2006; Livage, Beteille, Roux, et al., 1998; Maruszewski, Streck, Jasiorski, et al., 2003; Niederberger & Pinna, 2009).

Sol-gel method generally involves these steps:

1. Hydrolysis of pre-starter
2. Alcohol or water condensation of active sol-gel types
3. Polymerisation
4. Gelling
5. Wetting
6. Drying
7. High heat application (sintering)

General chemical reactions of sol-gel process, enables control through the first material till the last in order to make a proper design and produce a determined phase (Li, Fries & Malik, 2004). The factors depending on this control are the used pre-starter, solvent and catalysts.

Because sol-gel process involves transfer of a liquid 'sol' phase to a rigid 'gel' phase, inorganic sols and gels are generally re-produced through resolved chemical reactant synthesis in a liquid environment (Locher, Romano & Weber, 2005; Pierre, 1998). The reactant that involves a metal cation in an inorganic sol or gel is usually named as a chemical pre-starter. The chemical transformation of this structure is quite

complex. Similarly, transformation of sol to gel involves complex reactions in molecular level. These reactions also enable control of distribution of dense colloidal particles in sol and their agglomeration in gel (Pierre, 1998). Components used in sol-gel process are grouped as:

Whole resolvable pre-starters are used in sol-gel application. These may be under two main groups. Metal salt and alkoxides (Kloskowski, Pilarczyk & Chrzanowski et al., 2010; Pierre, 1998)

a) Metal Salts

The general formula of metal salts is M_mX_n . Here, M is metal, X is an anionic group, m and n are stoichiometric constants.

b) Metal Alkoxides

Alkoxides are defined as $M(OR)_n$ formula. Because metal alkoxides contain high electronegative OR group, they join reactions actively. These compounds are reactive when there is humid, heat or light. Unlike metal salts, the unpureness they create is because of organic groups (Pierre, 1998).

When choosing solvents, because the solvent chemistry of metal salts and metal alkoxides is different, choices should be made according to the type of pre-starter. Solvent may be water or organic kind of solvent. Because alkoxide and water do not mix with each other, there is a need for a proper solvent in sol-gel process in order to have a reaction. Water for metal salts and alcohol for metal alkoxides are used as solvents.

Alcohols like CH_3OH (methanol), C_2H_5OH (ethanol), C_3H_7OH (propanol), C_4H_9OH (butanol) are used in sol-gel method as starter material and react with metal oxides. Because water has an important effect in sol-gel process, it is defined differently from alcohols. In comparison with other parameters, water is a compound that directly join

(heat, parameters, catalyst) chemical reactions and constitute molecular structure. Stoichiometrically giving less water than needed to slow reaction down shows how important it is in sol-gel process (Pierre, 1998; Thitinun, Thanabodeekij & Jamieson et al., 2003). The amount of water in sol-gel process is define and evaluated with water/alkoxi ratio.

The catalysts used in sol-gel method are divided into two as acid and base (alkali) catalysts that belong to commonly used acid groups; acetic acid as organic, nitric acid as inorganic, hydrochloric acid and hydrofluoric acid. As base (alkali), ammonium hydroxide is one of the most used catalysts.

2.2.1.1 Hydrolysis

Hydrolysis is the deprotonation of a solvated metal cation. It consists in the loss of a proton by one or more of water molecules that surround the metal M in the first solvation shell.

As a consequence, the aqua ligand molecule, H₂O that is bonded to the metal is either transformed into an hydroxo ligand, OH⁻, if only one proton leaves or onto an oxo ligand, O²⁻, if two protons detaches. (Figure 2.4) (Niederberger, Pinna, 2009; Wright, Sommerdijk, 2001)

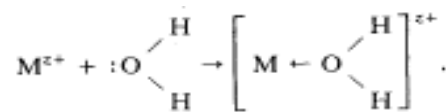
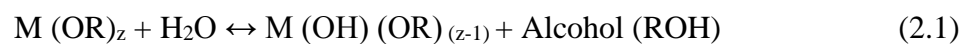


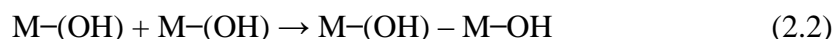
Figure 2.4 Hydrolysis process (Wright, Sommerdijk, 2001)

The reaction of hydrolysis can be expressed as follows:



2.2.1.2 Condensation

The first step is condensation by olation. The first step of any condensation reaction always includes the construction of an “ol” bridge in which a hydroxo ligand is caught between the two metal atoms. (Maruszewski et al., 2003)



The second step is condensation by oxolation. Condensation reactions between two hydroxylated metal species leads to M-O-M bonds under release of water (oxolation), whereas the reaction between a hydroxide and an alkoxide leads to M-O-M bonds under release of an alcohol (alkoxolation) (Figure 2.5) (Brinker & Scherer, 1990).

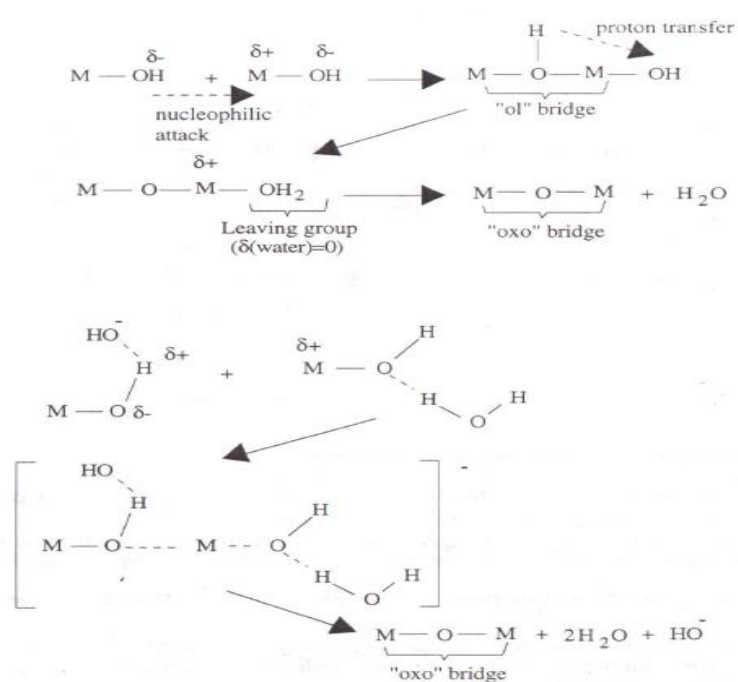
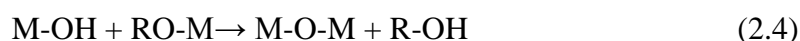
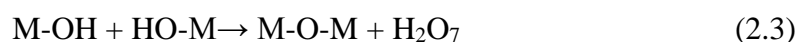


Figure 2.5 Condensation of olation and oxolation (Brinker & Scherer, 1990).

The reaction of condensation can be expressed as follows:



2.2.1.3 Polymerisation

Peptidisation is the process that precipitations are distributed with a resolvent. By distributing these precipitations, a sol is created. Electrolytes are the most appropriate materials in peptidisation. Electrolytes give a certain load of electric to particles. The reason why loading is a necessary is that colloidal particles are decisive only when they are loaded.

Peptidisation is a de-coagulation. However, coagulation is the process which colloidal particles deflect while increasing, because their electric load is zero. A precipitation is peptidised with OH⁻ ions (base) if they constitute a negative loaded colloidal precipitation and with H⁺ ions (acid) if they constitute a positive loaded precipitation (Figure 2.6) The amount of acid to add is configured with pH value of the environment (Brinker & Scherer, 1990).

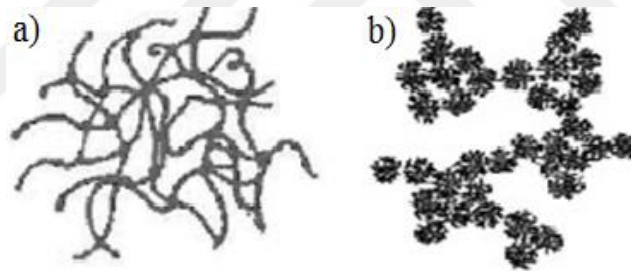
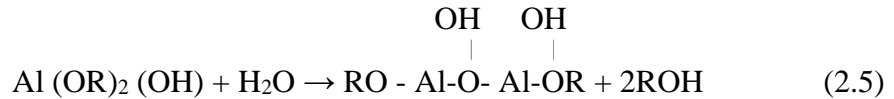


Figure 2.6 (a) The structure of acid catalyst mechanism (b) The structure of basic catalyst mechanism (Brinker & Scherer, 1990).

In order to determine the optimum point of acid/alkoxide ratio, acid is added gradually to test-tube. First a decrease and then again an increase is seen gelling point. The lowest point is the optimum point. Below and above acid amounts are high or low developed points. The decrease seen in gel volume is because there is the effect of acid particles on electric load.

When the amount of acid given rises, positively charged particles absorb anions and became neutral. Therefore, compressive force between particles decreases and they become closer, that is to say gelling volume decreases.

In addition to chosen acid amount, acid type is as important as acid amount which effect peptonisation. The ionisation constant of acids which not support peptidisation is below 1.10^{-4} . Because the acid concentration is too low, to have an electric force effect, the acid must be very strong. This rule, except for some strong acids, leaves other organic acids out (Li, Fries & Malik, 2004; Pierre, 1998; Znaidi, 2010).



After peptidisation and polymerisation phases, there is nucleation, after nucleation there is growing steps process occurs (Figure 2.7).

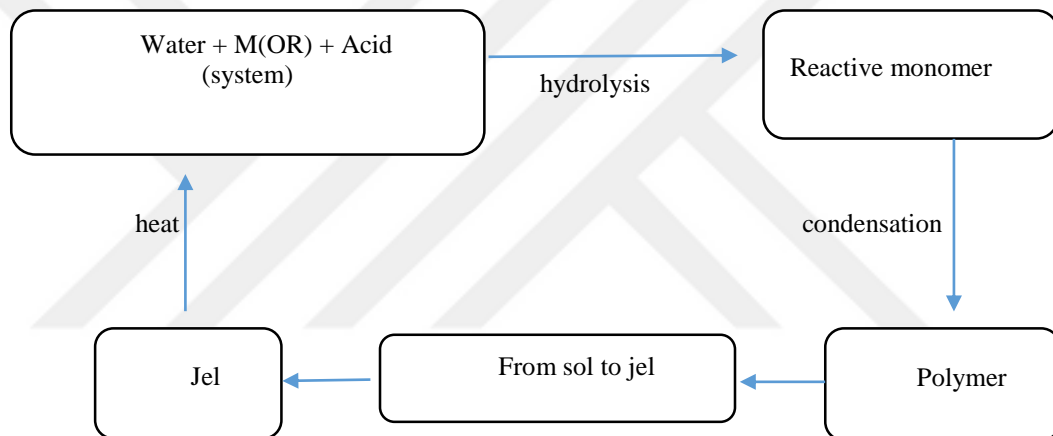


Figure 2.7 Polymerization (Li, Fries & Malik, 2004; Pierre, 1998; Znaidi, 2010)

There are also affecting factors in this process like:

- The nature concentration of pre-starter
- The type of resolvent
- Acidity of the environment
- Concentration of all types resolvent,
- Types and concentration of additives.
- Aging time of mixture
- Temperature
- Applied heat treatments (Li, Fries & Malik, 2004; Pierre, 1998; Znaidi, 2010)

2.2.1.4 Gelation

Gelation may be defined as the process that liquidity of a solution suddenly disappears, changes into an elastic rigid look-like. Depending on the speed and type of gelling reactions, micro structure of product, thus composed gels can be controlled.

As result of hydrolysis and condensation, clusters grow to bound together to create gel. Depending on the ability of being irreversible or reversible, rigid phase bounds, gels may be defined as weak or strong.

Gelling is simply defined as the agglomeration of particles until collision of clusters or growing of clusters by condensation of polymers and then bounding between clusters in order to constitute one big cluster. As a result of these processes the thing we call “gel” is produced.

These big spreaded clusters comprise the container they are in, so when the container is rolled the gel won't spill. In this moment, gel is produced; some of the spreaded but not bounded clusters are in the sol phase; in time, these become bounded gradually with the bond and enhance the stiffness of the gel. Accordingly, in order to constitute branched cluster, when the last bound occurs between two big clusters, gel is produced. This bound, in addition to being responsible from the first step of elasticity by constituting a constant rigid bound, is no different from the other numerous bounds which are constituted before or after gelling point. The occurred bond arc limits the influx of porous liquid. However, no exothermic or endothermic component occurs. The chemical development of the system is not affected (Brinker & Scherer, 1990).

Gelling point is defined as the point that rigid mass become connected in the beginning phase of polymerisation (Aurobind, Amirthalingam & Gomathi, 2006). This situation that occurs with condensation become clear by the increase of the viscosity of solution (Brinker & Scherer, 1990). For example, cyanol functional groups on the surface of growing particles surface during gelling synthesis of SiO₂ are molecules

that lost one or some protons and in order to keep sol in balance negative loads of these molecules act as pushing barrier.

Afterwards by vaporisation of solvent and hydrolysis of alkoxyan, water is consumed, contracted solution and unstable-indecisive suspension occurs. As a result, the rigidity of the product rises (Aurobind, Amirthalingam & Gomathi, 2006).

Because the size and shape of the last product is determined in gelling phase, it is important to control this phase. In order to have low condensation and porous product, gelling time must be one of the most important parameters of process. It is known that condensation of particles rises as gelling time rises (Figure 2.8). It is also emphasized that if the pH degree of sol is low, gelling time takes longer (Siouffi, 2003; Thitinun, et al., 2003)

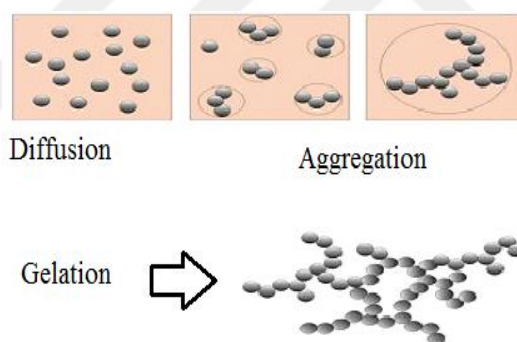


Figure 2.8 Gelation (Brinker & Scherer, 1990)

2.2.1.5 Aging

As the viscosity rapidly increases, the solvent is “trapped” inside the gel. The structure may change considerably with time, depending on pH, temperature and solvent. The gel is still “alive”. The liquid phase still contains sol particles and agglomerates, which will continue to react, and will condense as the gel dries. The gel is originally flexible. groups on neighbouring branches will condense, making the gel even more viscous. This will squeeze out the liquid from the interior of the gel, and shrinkage occurs. This process will continue as long as there is flexibility in the gel.

Hydrolysis and condensation are reversible processes, and material from thermodynamically unfavourable points will dissolve and precipitate at more favourable points (Note the similarity to the sintering process).

Long term wet gel aging before the last drying is important for achieving xerogel that is stable during storing phase. Until now, wet aging time wasn't accepted as a variable that affect outcome features of xerogel and this parameter was neglected frequently in the academic literature.

Morpurge and his friend mentioned that in reality these parameters are important and added that if aging does not occur until a certain stage, there probably won't be any further condensation reaction and the features of the last product may change significantly unexpectedly.

Aging in room temperature is a rather slow process and its speed depends on formulation in order to fasten aging process catalyst addition can be made. A catalyst addition into gelling mixture, may enable achieving a stable featured matrix in application time, namely it is compatible with practical usage (Keshmir, Troczynski, Mohseni, 2006).

In the last phase of gelling, water and organic solvents vaporise in the gaps of glass and the volume of rigid matrix crinkles gradually. In drying phase, while smaller pores stay wet with solvent, some bigger pores are empty. A porous glass-like rigid called "xerogel" is achieved as a last product (Aurobind, Amirthalingam & Gomathi, 2006).

2.2.1.6 Drying

When the liquid is removed from the gel several things may happen. When the liquid in the gel is replaced by air, major changes to the network structure may occur. If the structure is maintained, an aerogel is formed if the structure collapses, a xerogel is formed.

Normal drying of the gel leads to structural collapse due capillary forces drawing the walls of the pores together, and reducing the pore size.

- •OH groups on opposite sides may react and form new bonds by condensation.
- •Cracking may occur when the tension in the gel is so large that it cannot shrink anymore.
- •Gas will enter the pores with a thin film of liquid on the walls. This will evaporate and only isolated spaces with liquid are left.

Drying process of a porous material may be divided into two. First; the body shrinks equally with vaporised liquid volume and the water-steam surface stays outside the outer surface of the body. When the body harden too much to shrink, second phase begins and the water leaves the air-filled pores that are close to the surface and retreats into inner position. While the air takes hold of pores, a continuous water film supports the outer flow, so vaporisation keeps occurring from body surface. As a result, water is captured inside the pores and the drying may continue with diffusion of steam and vaporisation of water inside the body.

Drying of sol-gel is one of the critical phases. Drying is controlled via capillary pressure. Shrinkage occurs in gel in drying because of the capillary pressure and that pressure inside pores may cause a mechanical damage. A capillary tension during drying way reach 100-200 MP. In this case, it may result in shrinkage or fraction.

The last gel product, may contain hydroxyl and organic remnants. In order to create a really inorganic system, remnants must be destroyed. So as to destroy pores while volatile materials inside the pores are ejected, gel starts swelling and this causes deformation of the gel (Jones, 1989).

A tension between the liquid and the steam is inevitable in room temperature drying. The tension inside gel is proportional with drying pace and viscosity of pore liquid, is inverse proportional with the permeability of wet gel. Important parameters are the first phase of gel endurance, the pore size of wet gel and the resolvent used in drying.

Small pore size may cause fractions during drying because of the great amount of capillary force. When the pore size is smaller than 200 Å, pore liquid is under great tension. On the contrary, when there is a pore size bigger than 200 Å, there is less shrinkage and less possibility of fraction. In return, in some cases that can be explained with cavitation theory, gels with smaller sized pores (40 Å) are dried easier than bigger sized pores. An intervention can be made by drying solvent in size distribution (Siouffi, 2003).

If we think of pores in gel as nanometre-like hairline tubes, the liquid inside it is under hydrostatic pressure. The smaller the diameter of a hairline, the more the liquid inside it is under hydrostatic pressure. The smaller the diameter of a hairline, the more the liquid rise in tube because of liquid pressure. If the diameters of pore in gel are nanometre sized, the hydrostatic pressure would be higher. Thus, gels that have smaller pores shatter easily (Brinker & Scherer, 1990). Besides, two adjoin different sized pores may lead to a rise in pressure difference and in fractions.

Depending on one of the most important phase in sol-gel process the drying process, gel is produced in three different forms; aerogel, xerogel and criogel. Aerogels that achieved by supercritical drying are usually low-condensated and monolithic materials (Clapsaddle, Sprehn, Gash, Satcher, Simpson, 2004). Xerogels, on the other side, are achieved by drying approximately in room temperature and atmospheric pressure. Articles comparing these two materials and their efficiencies are available in academic literature (Jones, 1999; Hirashima et al., 1998; Maldonado-Hódar, Moreno-Castilla & Rivera-Utrilla, 2000).

Except from supercritical drying and traditional drying, alternative methods like freezing drying and microwave drying are also used in solvent exile from gels. It is known that dried gels, whose solvents were generally exiled by freezing drying have bigger pore volume comparing with the ones that were dried with conventional evaporation (Dilsiz & Akovali, 2002). Articles that research microwave drying are also in the academic literature (Zabova, Sobek, Církva, Solcova, Kment & Ha'jek, 2009).

2.2.1.7 Sintering

Sintering temperature, pace and environment have significant effects on the structure of last product (You, Chen, Zhang, 2005; Luis, et al., 2011). These affects were examined in the academic literature in every material one by one. One of those examinations belong to Porkodi and Arokiamary. By preparing nano-sized crystals with sol-gel method, they achieved calcine in 300 °C, 400 °C and 500 °C. The last crystals were characterised by XRD, TGA/DSC, FTIRman, SEM/EDX analysis (Porkodi & Arokiamary, 2007).

Different from classical calcination significant microwave calcination researches have been mode recently. The reason why they are trendy these days is that by traditional method, the heat can only be applied on the outer surface of materials however, by microwave, they can be heated from inner and outer cores of material and their photocatalytic activity features can be enhanced. It is also stated that heating via microwave depends on absorption capacity of material to heat (Addamo et al., 2008).

2.3 Spin Coating

2.3.1 Spin Coating General Theory

Spin coating process normally involves the application of a thin film (a few nm to a few um) evenly across the surface of a substrate by coating (casting) a solution of the desired material in a solvent (an "ink") while it is rotating.

End of the film thickness and other features will depend on the nature of the resin (viscosity, drying rate, percent solids, surface tension, etc.) and the parameters chosen for the spin process. Factors such as final rotational speed, acceleration, and fume exhaust contribute to how the properties of coated films are defined (Hellstrom, 2007; Mitzi et al., 2004). A machine used for spin coating is called a spin coater, or simply spinner (Figure 2.9).

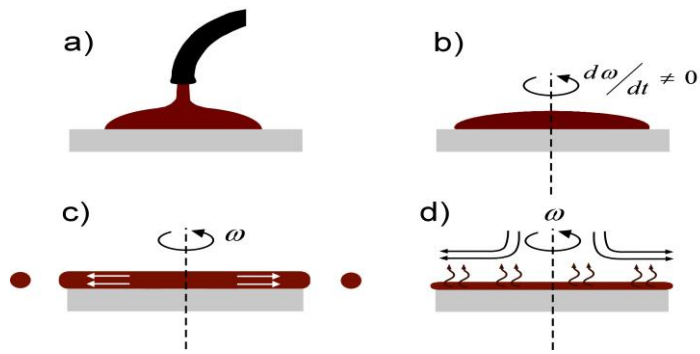


Figure 2.9 Four distinct stages to spin coating (Hellstrom, 2007)

Spin coating is widely used in micro-fabrication, where it can be used to create thin films with thicknesses below 10 nm. It is used intensively in photolithography, to deposit layers of photoresist about 1 micrometre thick (Hanaor et al., 2011). Photoresist is typically spun at 20 to 80 revolutions per second for 30 to 60 seconds. Owing to the low values of thickness which can be achieved using spin coating methods, this method is often employed in the fabrication of transparent titanium dioxide thin films on quartz or glass substrates, such thin film coatings may exhibit self-cleaning and self-sterilizing properties (Hanaor et al., 2011).

2.3.2 Description of Spin Coating Process

In many areas of organic electronics and nanotechnology the casting and drying stages of an ink are an integral part of the technology and is where all the "action" happens. Tyona 2013 research shows that spin coating processes are four distinct stages to the spin coating process (Figure 2.10). These include:

1. A dispense stage
2. Substrate acceleration stage
3. A stage of substrate spinning at a constant rate and fluid viscous forces dominate fluid thinning behaviour
4. A stage of substrate spinning at a constant rate and solvent evaporation dominates the coating thinning behaviour

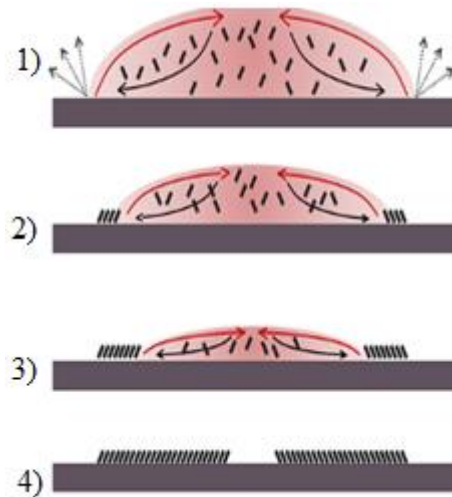


Figure 2.10 Drop casting slowly without rotation is a good way to provide highly ordered films at the nanoscale but at the expense of uniformity across the substrate.

Figure 2.10 shows how drop moves on the surface area;

- A small molecule in a solvent is first dispensed across the substrate and as the solvent begins to evaporate this produces internal currents (1).
- The droplet shrinks in size with the internal currents depositing molecules at the receding edges (2).
- By slowing down the evaporation rate it is possible to have highly ordered films produced at the edges (3).
- However, the coating across the surface is usually high uneven with a typical "coffee staining" effect (4).

By spin coating at very low speeds it is possible to get a combination of the high levels of nanoscale order produced by drop casting with the uniformity of spin coating. (Tyona, 2013)

2.3.3 Spin Coating Thickness Equation

If thin film is produced by spin coating technique, firstly it must calculate thickness of spin coated film. In general, the thickness of a spin coated film is proportional to

the inverse of the spin speed squared as in the below equation where ‘ t ’ is the thickness and ‘ w ’ is the angular velocity; (spin coating thickness equation at 2.6).

$$t \propto \frac{1}{\sqrt{w}} \quad (2.6)$$

This means that a film that is spun at four times the speed will be half as thick. A spin curve can also be calculated from this equation such as the below. And this equation shows how example spin curve occurs (Figure 2.11).

The exact thickness of a film will depend upon the material concentration and solvent evaporation rate (which in turn depends upon the solvent viscosity, vapour pressure, temperature and local humidity) and so for this reason spin thickness curves for new inks are most commonly determined empirically.

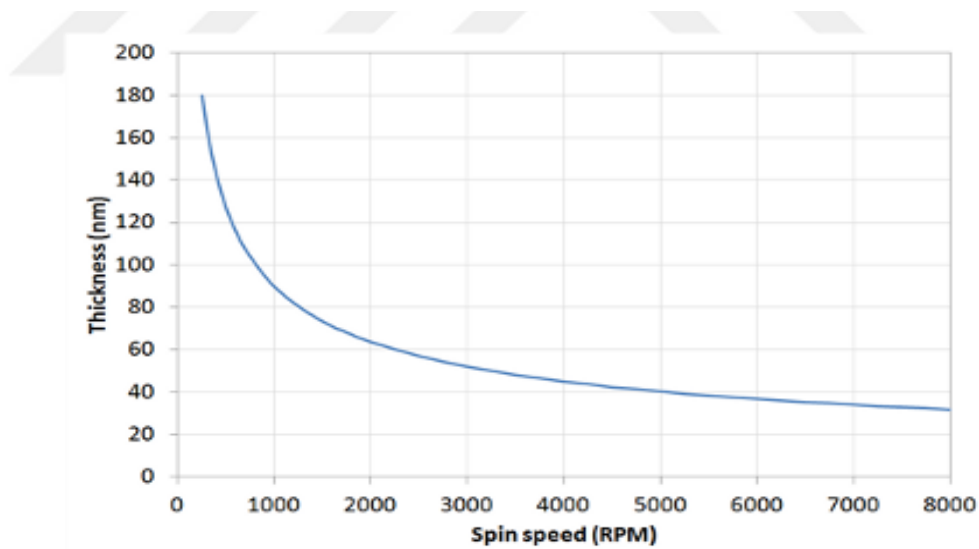


Figure 2.11 Example spin curve for a solution (Peeters & Remoortere, 2008)

Typically, a test film is spin coated and the thickness measured either by ellipsometry or surface profilometry. From this one or more data point(s) the spin thickness curve can be calculated - usually with a good degree of accuracy. The spin speed can then be adjusted to give the desired film thickness. Especially get a high

quality and consistent thin film the below points must be observed (Peeters & Remoortere, 2008).

- The substrate should have reached its desired rotational speed before the dispense happens (usually only a few seconds).
- The ink should be deposited as close to the centre of the substrate as possible otherwise you may end up with a gap in the middle.
- The ink should be deposited in one quick and smooth action.
- The ink should be deposited in one and only one drop in order to prevent multiple coats.
- There should not be any bubbles blown onto the surface from the pipette.

Huang & Chou (2003)'s study shows; as the feature dimension of ultra large-scaled integration technology continues to shrink, interconnection delay, generally termed resistance-capacitance (RC) time delay, dominates most attention over the basic gate delay in the deep submicron devices. Therefore, insulating materials with low dielectric constants are needed to mitigate this problem of RC delay and cross talk between metal interconnects. Sol-gel derived porous SiO₂ xerogel film is particularly attractive among various low k dielectric candidates in advanced semiconductor devices, because of its inherent ultra-low permittivity and high thermal stability through the incorporation of micropores into the SiO₂ skeletal network.

Spin coating is a simple and reliable process for depositing uniform coatings onto flat substrates. As with all chemical and manufacturing processes, great care must be exerted to ensure that high quality products are made. For spin coating this means that careful understanding of the solvent evaporation and drying characteristics must be achieved. And, some of the details of the flow behaviour of the solution are important too. Because of the complexity of some sol-gel solutions (Aegerter & Mennig, 2004).

CHAPTER THREE

EXPERIMENTAL

3.1 Purpose of Thesis

The main idea lying under neurostimulator systems are, converting received signal through converters and modulators into necessary amplitude according to desired area. The main purpose of empirical studies to conduct is to complete this conversion and to stimulate nerve cell successfully.

Calling this system, a successful system depends on its efficiency of activation and inhibition with the electronic system on it. Suitable material selection to conduct a working neurostimulator Project is the main priority of this thesis.

Detailed information was given on semi conductive plate that a neurostimulator has to have, necessary features and performance of thin film plate. Here, in addition to characteristical features, dielectric constant is also of great importance.

The purpose of this thesis is comparing materials from dielectric point of view, in order to coat on semi-conductive silicon wafer. The materials were chosen among Al_2O_3 , TiO_2 as metal oxide, PVA, PMMA as polymer and producing sol-gel and spin coating method. Analysis of finished coatings literately and quality-performance association.

Effecting factors during production stage are characterization and optimization of produced materials, evaluation of achieved dielectric estimations.

Thus, appropriate material selection for neurostimulators using sol-gel and spin coating techniques, showing the effects of dielectric constant and performance on neurostimulator performance. It can be used with the dielectric performance for neurostimulator devices.

3.2 Materials

3.2.1 Substrate Preparation

In order to achieve single crystal silicon ingot, one of the most used techniques in the world the Czochralski technique, was applied using PVA Tepla Czochralski single crystal ingot growing device in Elektronik Malzemeler Üretimi ve Uygulama Merkezi (EMUM) at Dokuz Eylül University (DEU).

The steps depend on lengthening polycrystal particles in quartz pot (melting above the melting temperature of polycrystal silicon) and lengthening of core crystals, which have intended tendency, with determined spin speed and lengthening speed. Thus, ingot is achieved.

3.2.1.1 Silicon Single Crystal Growing

5 kg of polycrystalline silicon is loaded into the system. Melting temperature is determined as 1429 °C and from that point on, it is lengthened with speed of 1.1 mm/min and spin speed (crystal/pot) is determined as 10/10 spin/min. Argon gas influx speed during the process is configured as 25 L/min (Table 3.1).

Table 3.1 Silicon single crystalline

Parameters used in the body stage	The values in the recipe
Diameter	100 mm
Crystal Length	200 mm
Average Pulling Speed	1.1 mm/min
Rotation Rate (Crystal /Cupel)	10/10 per/min
Argon (flow / pressure)	25 (L/min) / mbar

Single crystal ingot production process lasted around 19 hours, and 200 mm long, 90 mm wide ingot was produced (Figure 3.1).



Figure 3.1 PVA Tepla Czochralski single crystal ingot and wafer

PVA Tepla Czochralski single crystal ingot of Si production process is showed in Table 3.2.

Table 3.2 The numerical result of Si single crystal

Si Single-Crystalline Results	Units
Single Crystal Body Length	200 mm
Average Diameter (Real)	90 mm
Average Diameter (Software)	100 mm
Body Phase Average Pulling Speed	1.1 mm/min
Leakage Ratio	8×10^{-4} mbar. l/s
Total Enlargement Time	≈ 19 hour

3.2.1.2 Silicon Ingot Slicing Process

Parameters of STX-1202 slicing device in the project like tambour speed, coating liquid flow and progression speeds of x, y, z towards ahead are optimized and the best values of single crystal ingot slicing is determined (Figure 3.2).

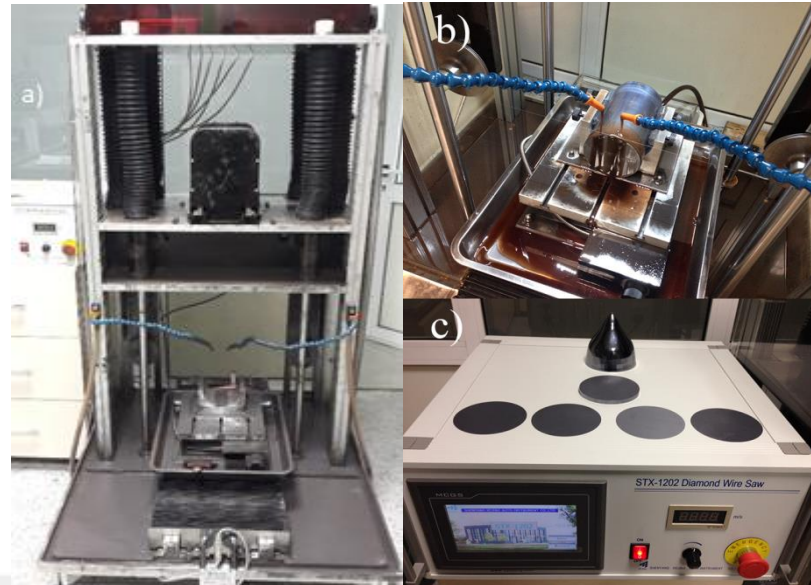


Figure 3.2 STX-1202 slicing device and slicing process

The expected wafer thickness during slicing process is determined as 1 mm. First, the produced silicon ingot is placed on cutting bench and the cutting speed is fixed as 3.5 m/s to have 1 mm slice in a minute. Thus, surface destruction is kept minimum with this cutting pace.

The reason why the sliced wafers are lapping/polished is that the surface that will be coated is needed to be smooth and bright. In order to apply nanoelectronic processes, the best surface that is needed are smooth and bright surfaces.

3.2.1.3 Lapping & Polishing Process

In order to apply wafers into lapping/polishing and slicing processes, they must be stabled on a glass base. So as to do that, the wafer is pasted on a 140°C heated glass base by a polymer and to have a good pasting, it was left to cool by placing a load on it in order not to let a gap occur between the glass and wafer.

Then, the wafer that was ready to be polished, was placed on the device to polish. Surface quality was made periodically and was controlled in order to check if they have same level of smoothness at each point (Figure 3.3).



Figure 3.3 Slide silicon ingot lapping process

In lapping and polishing processes, cerium oxide powders, silica suspension and alumina powders were used. At the end of the process after necessary polishing was made, slicing process was conducted (Figure 3.4).

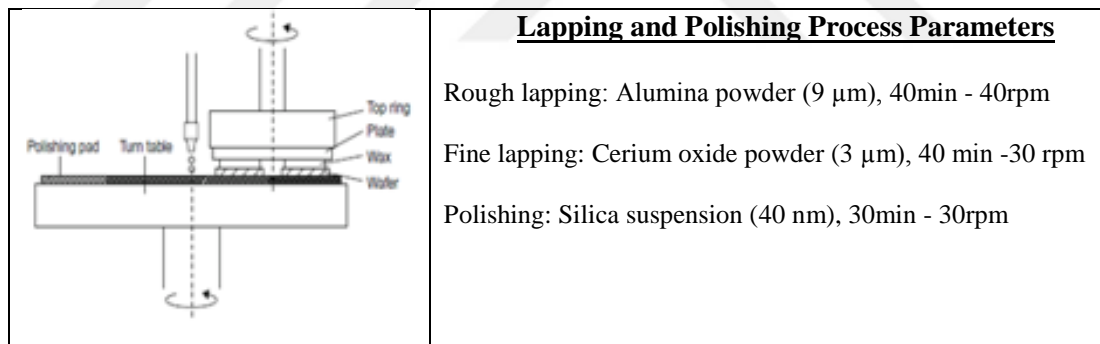


Figure 3.4 Lapping and polishing process parameters

3.2.1.4 Silicon Ingot Cutting Process

In this step, the sample that was ready for cutting, was rendered into small pieces of 1x1 cm or 2x2 cm square parts. After placing the device properly, necessary configuration was made to make samples ready for coating. Spinning speed of device was adjusted as 2300 rpm and feeding speed of sample was 0.25 mm/sec. (Figure 3.5-3.6).



Figure 3.5 1x1 cm and 2x2 cm samples for cutting process

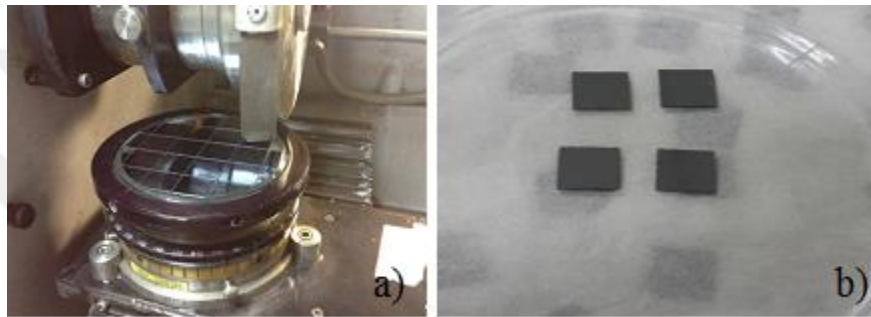


Figure 3.6 (a) 2x2 cm and (b) 1x1 cm cutting wafers

The results of applications that were made with micro-structural characterisation and scanning electron microscope (SEM) and EDS. Analysis results were given in Figure 3.7 and 3.8. As a result, in order to examine micro-structural features of silicon chips, SEM analysis's were made (Figure 3.7).

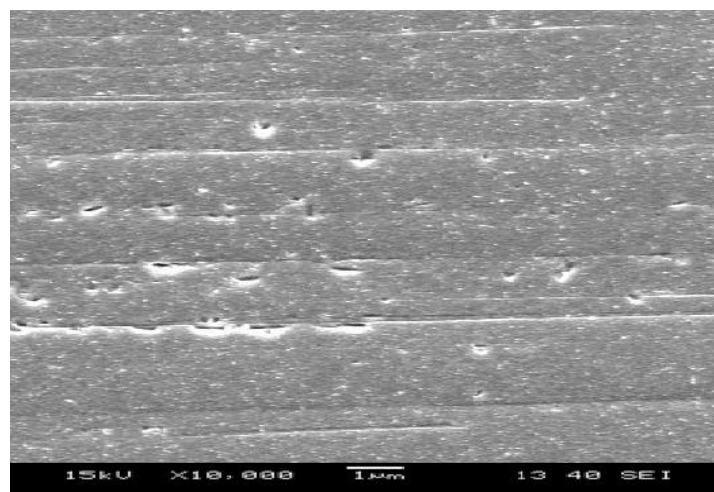


Figure 3.7 SEM results for pure Si

Si and C were found in structure after EDS analysis (Figure 3.8). The C found in analyses are rooting from the carbon bond that was used to paste silicon sample. As a result of the analysis, it is determined that the material was containing only silicon.

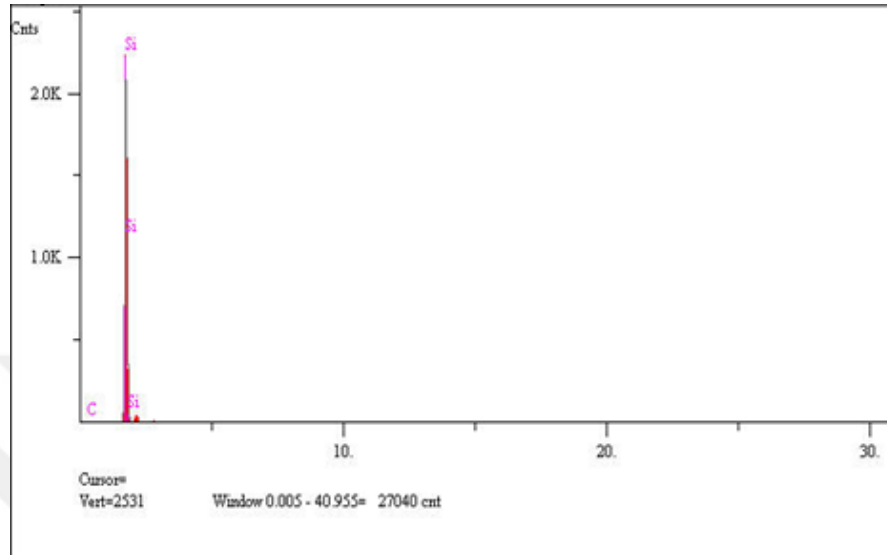


Figure 3.8 EDS results for pure Si

X-ray diffraction results were shown in Figure 3.9. In the characterisation application that were made with Si wafer material that were prepared inside structure, XRD analysis was made. The achieved results support SEM-EDS analyses result. There is only Si inside the structure.

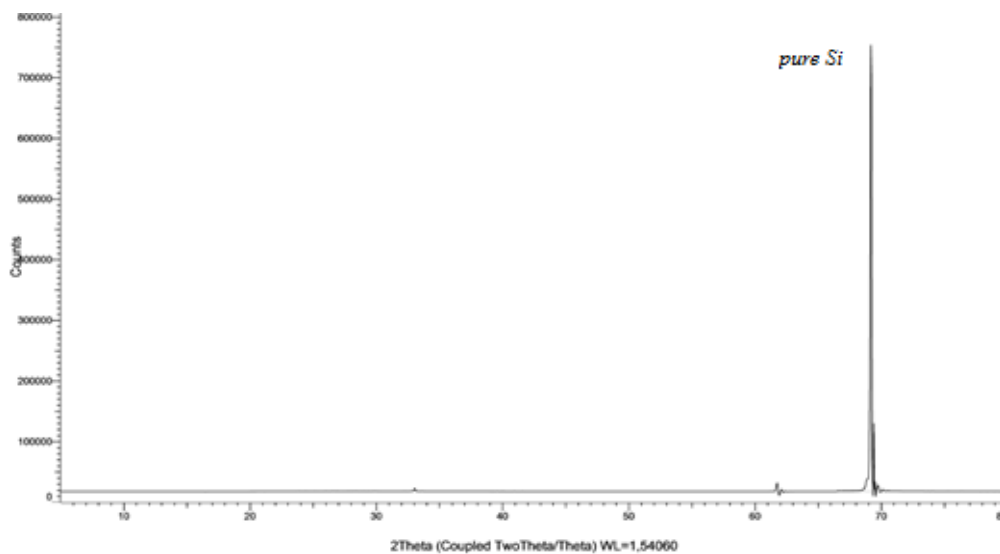


Figure 3.9 XRD pattern for pure Si

3.2.2 Solution Preparation

3.2.2.1 Preparing of Metal Oxide Groups Samples

In order to get crack, pinhole free and uniform thin films in the exact stoichiometry, homogenous solutions must be prepared. In this part there are two main solutions, these are Ti and Al based solutions. For Ti based solution Precursor solution was obtained by dissolving titanium (IV) isopropoxide ($\text{Ti}\{\text{OCH}(\text{CH}_3)_2\}_4$) in ethanol. The metal concentration of the solutions was set as 0.6 M. For Al based solution $\text{AlCl}_3 \cdot 6\text{H}_2\text{O}$ used as precursor. $\text{AlCl}_3 \cdot 6\text{H}_2\text{O}$ was dissolved in distilled water. GAA (Glacial acetic acid) was added into both two solutions until completing dissolution which was accomplished within few minutes. The solutions were stirred until the precursor was completely dissolved and a clear solution is obtained (Figure 3.10).

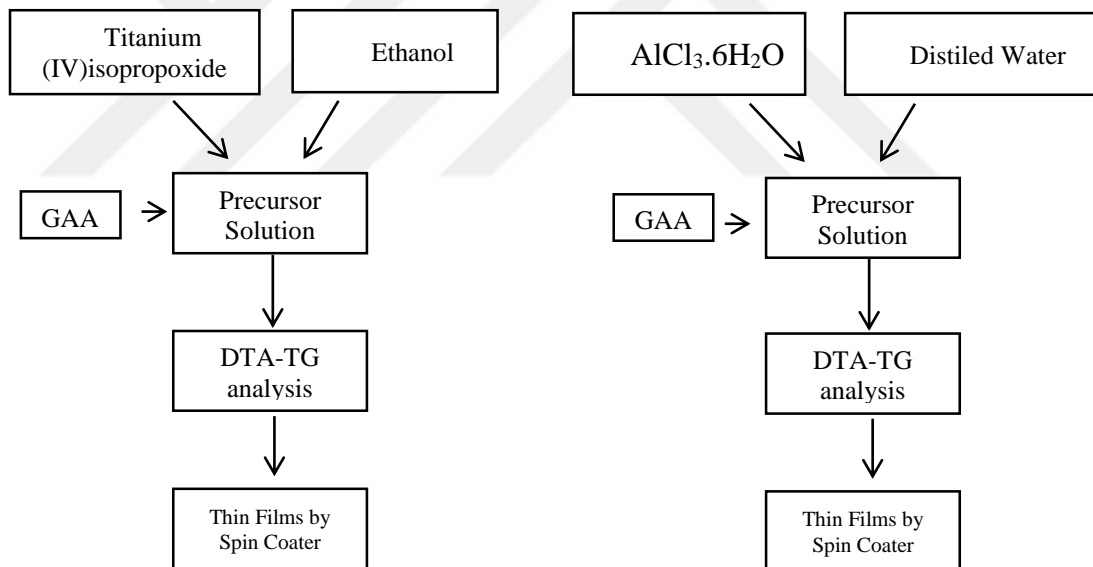


Figure 3.10 Flowchart for preparation of metal oxide samples

3.2.2.2 Preparing of Polymer Groups Samples

Also in this part there are two main solutions, these are PVA and PMMA based solutions 4 g hydrolysed PVA powders (*Aldrich*) were dissolved in 100 ml deionized water by heating 85 °C. 1 wt.% of Non-ionic surfactant Triton X-100 (*Aldrich*) was than mixed with PVA solution to get lower the surface tension. The hot solution was

stirred until the polymer was completely dissolved and a clear viscous solution is obtained. 4 g PMMA (*Aldrich*) were dissolved in 100 ml chloroform. The polymer solution was stirred until the polymer was completely dissolved and a clear viscous solution is obtained.

3.2.3 Spin Coating

3.2.3.1 Spin Coating Process for Metal Oxide Groups

The metal oxide based films were coated on the glass and Si (100) metallic substrates from the prepared suspension solutions through (POLOS-SPIN150i) spin coater. Different spinning parameters such as spinning rate, acceleration time were used to control the film thickness for two different films. The spinning rate of 4500 rpm for 50 seconds and an acceleration time of 10 seconds were used for metal oxide based films as optimal parameters (Figure 3.11).

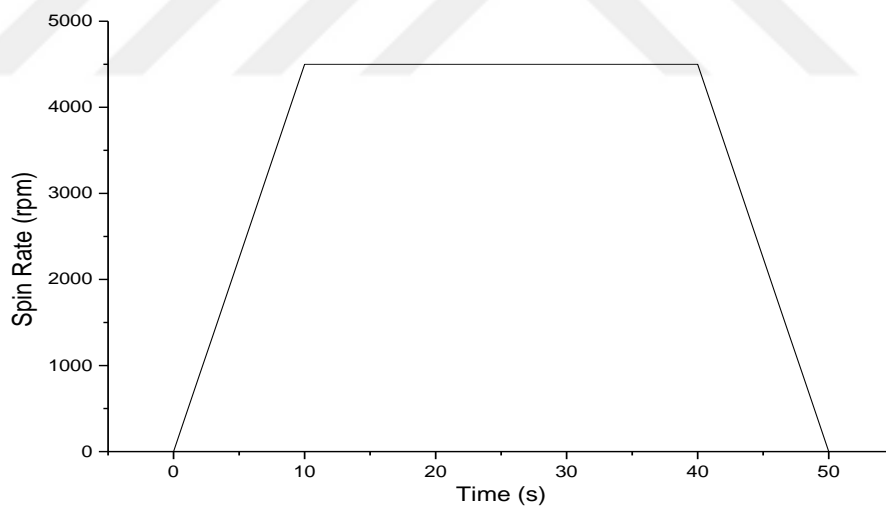


Figure 3.11 Spin rate/time schedule for metal oxide groups

3.2.3.2 Spin Coating Process for Polymer Groups

Likewise, metal oxide films, polymeric films were also produced by spin coater. Prepared polymeric solution with PVA and PMMA dropped Si wafer and spinning

best parameters were determined. For PVA solution, the spinning rate of 7500 rpm for 70 seconds and an acceleration time of 15 seconds were used (figure 3.12).

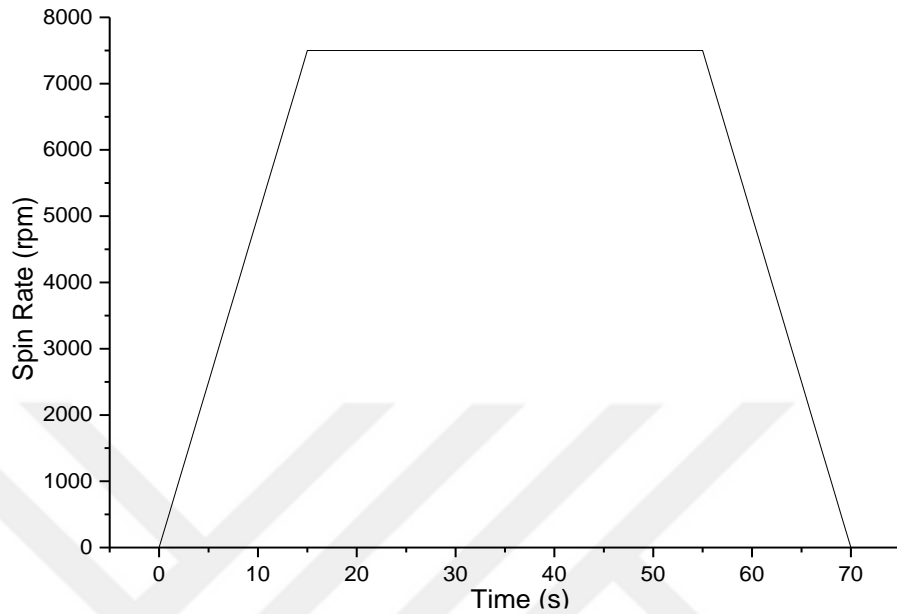


Figure 3.12 Spin rate/time schedule for PVA

However, PMMA solution was less viscos than PVA one, spinning parameter differs from it. Such as 5000 rpm spinning rate, 50 second spin time, 10 second acceleration time (Figure 3.13).

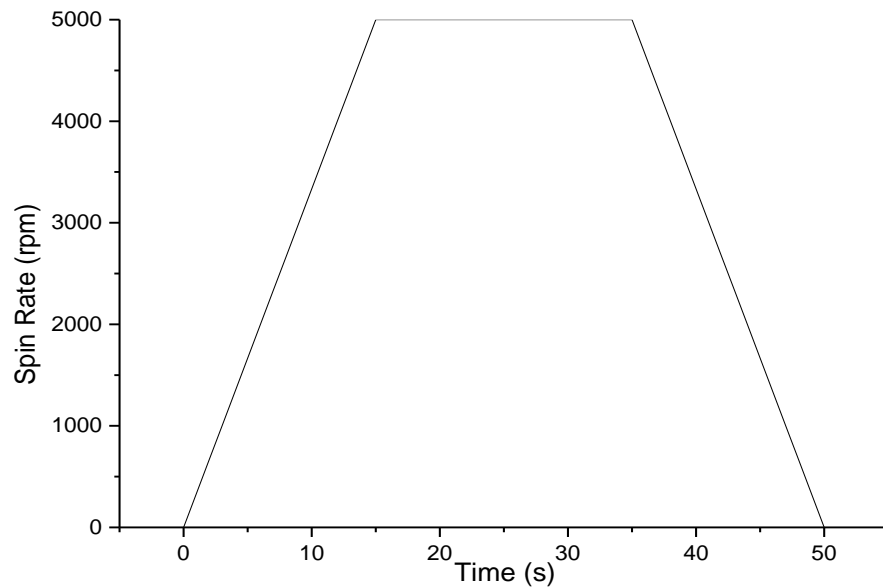


Figure 3.13 Spin rate/time schedule for PMMA

3.2.4 Heat Treatment

Because there are two type of sample, two different heat treatment regimes were used. The Protherm Furnace was effectively used for the calcining and annealing processes of metal oxide sample illustrated and polymeric samples were dried in an oven illustrated figure 3.14.

High temperature treatment was not employed for polymer based samples because of their typical decomposition characteristic at high temperatures.



Figure 3.14 Protherm (metal oxide group) and Nüve MF120 oven (polymer) for heating processes

3.2.4.1 Heat Treatment for Metal Oxide Groups

For the heat treatment regime of the TiO_2 samples, the temperature of the furnace was raised to $280\text{ }^\circ\text{C}$ with heating rate of $10^\circ\text{C}/\text{min}$ by nitrogenous atmosphere (N_2) and then kept at this temperature for 30 minute.

Then the furnace was raised to 450 with heating rate of $10^\circ\text{C}/\text{min}$ after it was kept at this temperature for 120 min, lastly it was waited until coming back to room temperature (Figure 3.15).

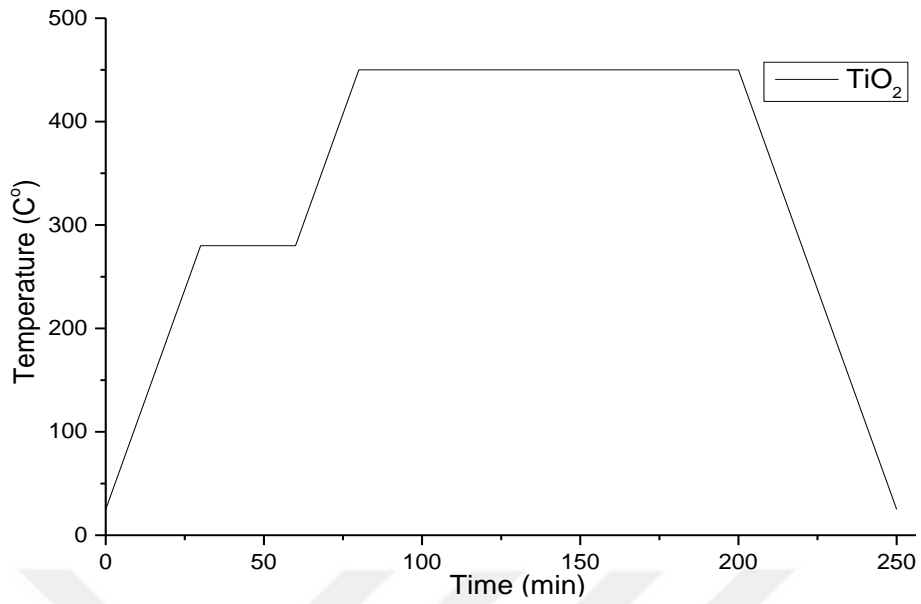


Figure 3.15 Heat treatment for TiO₂ of metal oxide group

Likewise, heat treatment regime of TiO₂, the temperature of the furnace was raised to 150 °C with heating rate of 10°C/min by N₂ and then kept at this temperature for 30 minutes for Al₂O₃ and then was raised to 250 °C with waiting 30 min. Then furnace temperature was raised 1000 °C kept at this temperature 120 min, finally it was waited in air until turning back to room temperature (Figure 3.16).

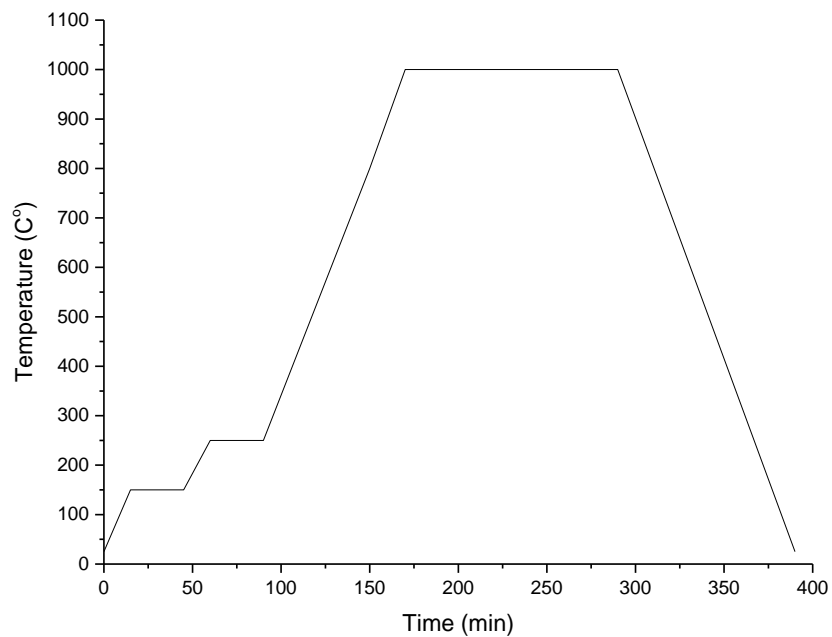


Figure 3.16 Heat treatment for Al₂O₃ of metal oxide group

3.2.4.2 Heat Treatment (Dehydration) for Polymer Groups

Because of low degradation temperature of polymer high temperature heat treatment was not applied to PVA and PMMA based samples. Aim of low temperature heat treatment was evaporation of water in solutions. After PVA and PMMA thin films were formed on Si wafer by spin coater equipment dehydration process was applied for both two films. Dehydration regimes were demonstrating in figure 3.17 and figure 3.18 for PVA and PMMA respectively.

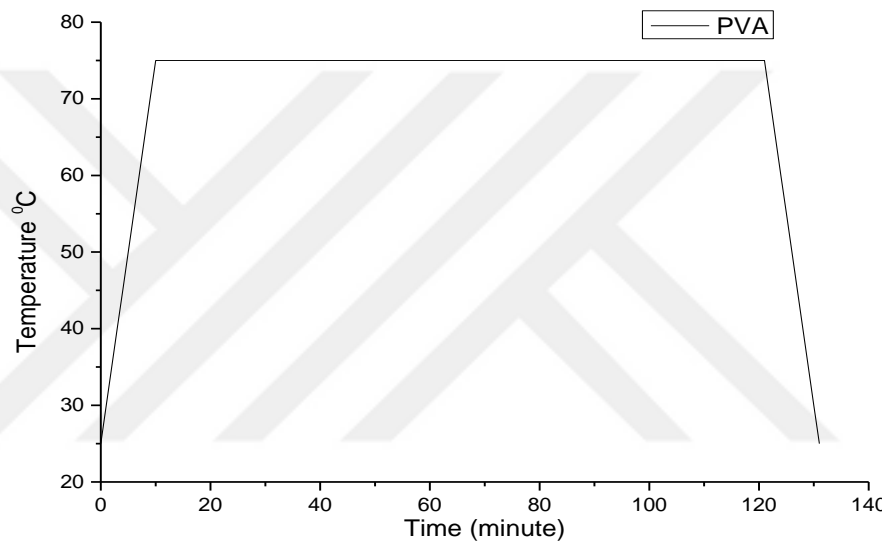


Figure 3.17 Dehydration regimes for PVA

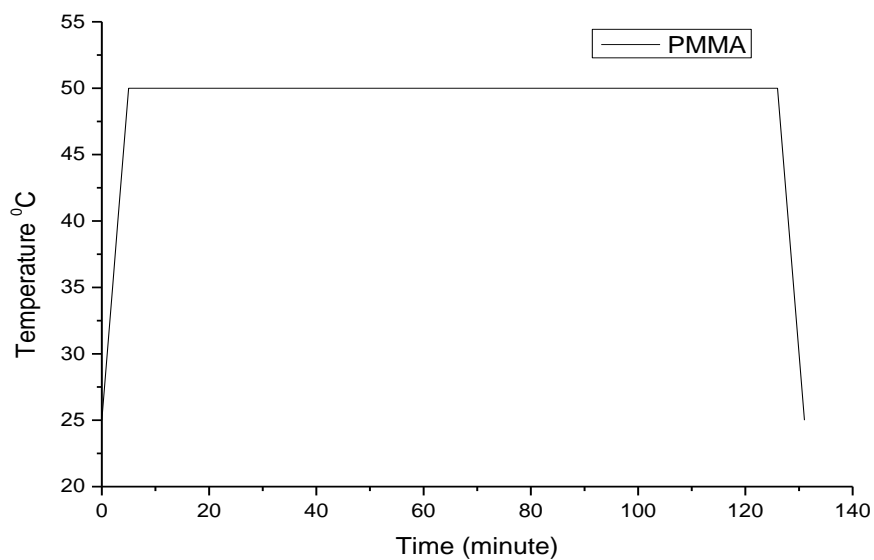


Figure 3.18 Dehydration regimes for PMMA

3.3 Characterization

3.3.1 Solution Characterization

To obtain optimum thin film or final particle properties different characteristic of solutions should be determined. For this aim various characterization studies were done.

3.3.1.1 PH Measurement

The pH measurement refers to determination of the activity of hydrogen and hydroxyl ions in an aqueous solution. Many important properties of a solution can be determined from an accurate measurement of pH, including the acidity of a solution and the extent of a reaction in the solution.

Many chemical processes and properties, such as the speed of a reaction and the solubility of a compound, can also depend greatly on the pH of a solution. In this study HANNA HI83141 pH meter was used to determine pH values (Figure 3.19).



Figure 3.19 HANNA HI83141 pH meter

3.3.1.2 Turbidity Measurement

Turbidity which means the relative cloudiness of a liquid, gives the optical characteristics of suspended particles in a liquid. Light is passed through the sample and is scattered in all directions. The light that is scattered at 90° angle to the incident light is then detected by a photo diode and is converted into a signal linearized by analyser and displayed as ntu. The more suspended particles there are in a liquid, the lighter will be scattered, resulting in a higher ntu value (Wilde & Gibs, 2002). In this study VELP TB1 turbidimetry was used to determine turbidity values (Figure 3.20).



Figure 3.20 VELP TB1 turbidimetry

3.3.1.3 Contact Angle

The contact angle is defined as the angle formed by the intersection of the liquid-solid interface and the liquid-vapour interface (geometrically acquired by applying a tangent line from the contact point along the liquid-vapour interface in the droplet profile). More specifically, a contact angle less than 90° indicates that wetting of the surface is favourable, and the fluid will spread over a large area on the surface; while contact angles greater than 90° generally means that wetting of the surface is unfavourable so the fluid will minimize its contact with the surface and form a compact liquid droplet (Yuan & Lee, 2013).

3.3.1.4 Fourier Transform Infrared Spectroscopy (FTIR)

Infrared spectroscopy can result in qualitative analysis of every different kind of material. By interpreting the infrared absorption spectrum, the chemical bonds in a molecule can be determined. In principle, molecular bonds vibrate at various frequencies depending on the elements and the type of bonds. For any given bond, there are several specific frequencies at which it can vibrate. FTIR spectrum of solution of TiO₂ and Al₂O₃ were recorded by using Thermo Scientific Nicolet iS10 model FTIR to determine the organic components in the samples. FT-IR absorption spectra were measured over the range of 4000 to 400 cm⁻¹ at room temperature (Figure 3.21).



Figure 3.21 Thermo Scientific Nicolet iS10

3.3.2 Materials Characterization

3.3.2.1 Differential Thermal Analysis-Thermal Gravimetric Analysis (DTA-TGA)

The thermal analysis of the gel was studied under N₂ flowing by means of PerkinElmer STA 6000 Model Differential Thermal Analysis-Thermal Gravimetry as shown in Figure X in order to obtain information about the decomposition behaviour of the gels and adjust the thermal treatment accordingly.



Figure 3.22 PerkinElmer STA 6000 Model Differential Thermal Analysis-Thermal Gravimetry

Thermal analysis is defined as a group of techniques in which a physical thermal analysis is defined as a group of techniques in which a physical property of the substance and its reaction products are measured as a function of temperature whilst the substance is subjected to a controlled temperature program (Hill, 1991). In addition to these, thermal methods are based upon the measurement of the dynamic relationship between temperature and some property of the system such as mass and heat absorbed by or evolved from it. Differential Thermal Analysis (DTA) and Thermogravimetry (TG) are the most important thermal methods used in characterization of materials (Kayatekin, 2006).

3.3.2.2 X-Ray Diffractometer

X-ray diffraction (XRD) is one of the basic techniques to analyse all kinds of materials such as powders and crystals and then XRD provide determinations about crystalline structure and structural phases (based on Bragg's Law that equation shown below). So Bragg's law provides the condition for a plane wave to be diffracted by a family of lattice planes.

$$n \cdot \lambda = 2 \cdot d \cdot \sin \theta \quad (3.1)$$

Where d is the lattice spacing, θ the angle between the wave vector of the incident plane wave, k_0 , and the lattice planes, λ its wave length and n is an integer, the order of the reflection. It is equivalent to the diffraction condition in reciprocal space and to the Laue equations (Figure 3.23).

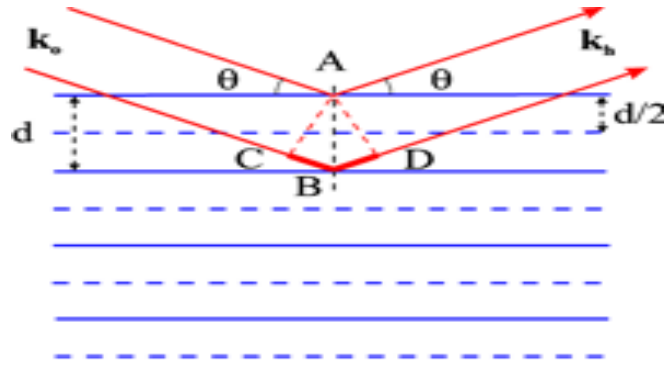


Figure 3.23 X-Ray Diffraction

In this step, XRD was used to analyse whether produced silicon ingot was single crystal or not. Pure silicon wafer, p-type silicon wafer and n-type silicon wafer were identified by means of XRD with a grazing angle attachment and an incident angle of 1° (Thermo-Scientific, ARL- K_α). X-Ray radiation of Cu- K_α was set at 45 kV and 44 mA with a scanning speed of $2^\circ/\text{min}$.

3.3.2.3 Scanning Electron Microscopy (SEM)

Scanning electron microscopy (SEM) is powerful instrument which permit the observation and characterization of heterogeneous organic and inorganic materials and surfaces on a local scale. In SEM, the signals of the greatest interest are the secondary backscattered electrons, since these vary according to differences in surface topography as the electron beam sweeps across the specimen (Goldstein et al. 1992). Series of radiations can be produced in terms of the interaction between the electron beam and the sample. Normally, two types of radiation are utilized for image formation: primary backscattered electrons and secondary electrons. Backscattered electrons reveal the compositional and topographical information of the specimen. The secondary electron images produce a depth of field which shows the surface topography. The signal modulation of the two types of radiation is viewed as images in the cathode ray tube (CRT) and provides the morphology, surface topology and composition of the specimen surface. In this study, the surfaces of pure, p- and n-type silicon wafer and texturing wafer were examined by using JEOL JSM-6060 instrument operating at an accelerating voltage of 20 kV with several magnifications.

3.3.2.4 Dielectric Measurement

Dielectric properties of metal oxide and polymer groups were determined using Novocontrol Alpha-N High Resolution Dielectric Analyzer (Figure 3.24). So dielectric constant was measured as dielectric parameters. Dielectric constant is the most important parameter for this thesis. Because of that material performance related with dielectric constant. It shows characteristic properties of material about electrical. This mechanism principle is that sample cells were utilized as a plate capacitor and the sample material was placed between two external capacitor plates as shown in Figure 3.24.

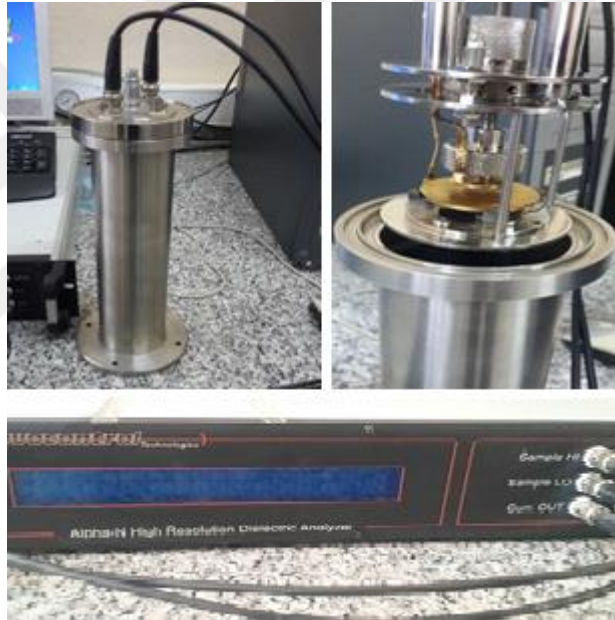


Figure 3.24 Novocontrol Alpha-N High Resolution Dielectric Analyzer

The material dielectric function is calculated by;

$$\varepsilon^* = \varepsilon' - i. \varepsilon'' = \frac{Cp^*}{Co} \quad (3.2)$$

from the measured complex sample capacity, Cp^* . Co is a constant determined by the sample geometry. Equation 3.2 refers to evaluation of data for details. Equation 3.2 will be only exact, if the electrical field distribution is homogenous inside the sample

capacitor and zero outside. In practice, there will be some field inhomogenitites at the capacitor borders reducing the sample capacity. In addition, the field outside the capacitor will not be zero. Instead there will be a stray field, which contributes as an additional external capacity to the measured sample capacity. Both contributions can be considered by an additional capacity which is edge capacity (C_{edge}). The measured capacity can be written as; (in which C_p^* is the capacity of the ideal capacitor).

$$C_m^* = C_p^* + C_{edge} \quad (3.3)$$

C_{edge} can be exactly calculated for round capacitor plates centred in an evacuated and grounded metallic sphere with infinite radius (capacitor not filled with sample material) (Vasilyeva, Lounev & Gusev, 2013). Dielectric measurement system is shown in Figure 3.25. This illustration includes a plate capacitor with the sample material and two external capacitor plates.

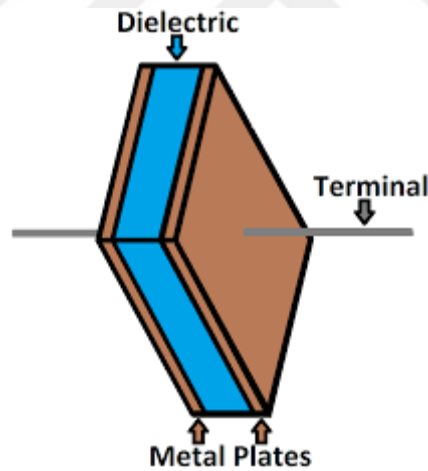


Figure 3.25 Dielectric illustration

CHAPTER FOUR

RESULT AND DISCUSSION

4.1 Solution Results

4.1.1 PH Results

The pH values of metal oxides groups the solutions were found as 4.65 (Al_2O_3) and 4.84 (TiO_2). The pH values of the solutions decreased as a function of acetic acid content in the solution. Their pH values are a significant issue to determine transparent solutions.

According to this result, acidity of the solutions does not change within first 15 minutes because they stabilize. It was estimated that the pH values of the solutions come to stable state. Since pH value of the solution is an important factor influencing the formation of the polymeric three-dimensional structure of the gel during the gelation process, it should be taken into consideration while preparing solutions. While ramified structure is randomly formed in acidic conditions, separated clusters are formed from the solutions showing basic characters (Ebelioglugil, 2009).

The other factor is dilution of the solution using solvent. The excess solvent physically affects the structure of the gel, because the liquid phase mainly consists of the excess solvent during the aging procedures. The changes in the gel structure at this stage partly influence the final structure (Ebelioglugil, 2009).

4.1.2 Turbidity Results

Most modern instruments measure 90° scatter and they are called nephelometric turbidimeter. Turbidity measured in this way is stated in nephelometric turbidity units (ntu). In the current turbidity measurements were performed using nephelometric ratio method and the obtained results were recorded in terms of ntu with ± 2 of value or ± 0.01 ntu accuracy. With turbidity experiments, whether powder precursor materials are

dissolved very well in solutions is understood by looking ntu values before coating process. As mentioned before, the turbidity values of the solutions vary in the range of 0 ntu and 1,000 ntu. It is interpreted that powder based precursors are completely dissolved as turbidity value approaches to 0 ntu and they are not dissolved and some powder particles are suspended in a solution as it approaches to 1000 ntu.

In this experiment, turbidity value of the metal oxide groups solutions was measured as 11.42 ntu (Al_2O_3) and 10.23 ntu (TiO_2). Also turbidity value of the polymeric groups solutions was measured as 3.17 ntu (PVA) and 3.02 ntu (PMMA).

Based on the turbidity value, it can be pointed that powder based precursors are completely dissolved in the solutions. Moreover, these values present an important clue for further processing. It is worth noticing that optimum structural, thermal, microstructural, mechanical, optical and high dielectric properties are not obtained using undissolved solutions.

4.1.3 Wettability Results

Wettability studies usually involve the measurement of contact angles as the primary data, which indicates the degree of wetting when a solid and liquid interact. Small contact angles (90°) correspond to high wettability, while large contact angles (90°) correspond to low wettability.

4.1.3.1 Determination of The Contact Angle of Metal Oxide Sample

Contact angle of aluminium oxide solution was made by double sided estimation. As a result, while the contact angle from left side was 7.27° , the right side was 4.32° . The contact angle determined by optimization was 5.80° . Hence, because the contact angle was below 90° , it is a solution with a great wetting capacity and it is appropriate for coating (Figure 4.1).

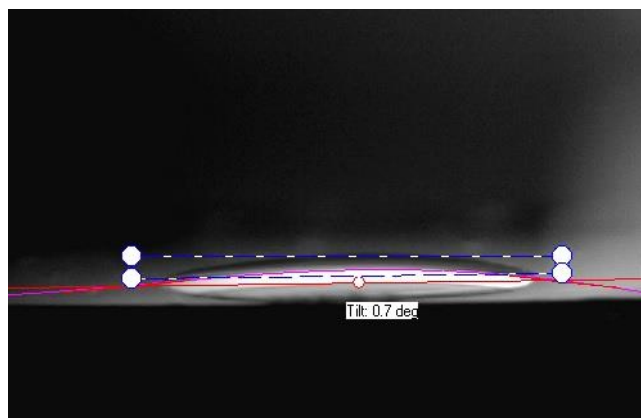


Figure 4.1 Al₂O₃ solution contact angle

Similarly, in the research made for titanium dioxide solution, while the left contact was 28.43°, the right side contact was 22.21°. The contact angle determined by optimization was 29.84°. Hence, similar to aluminium oxide solution, the wetting capacity can be classified as a high (Figure 4.2).

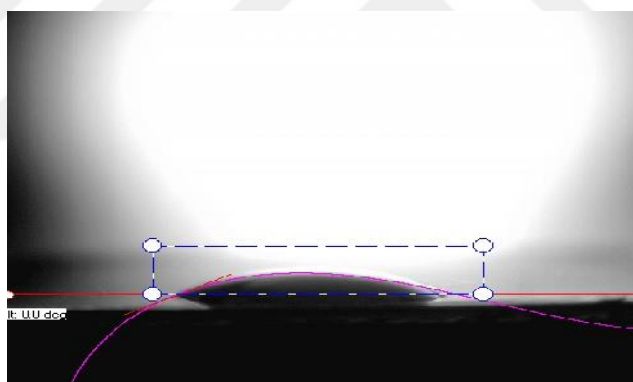


Figure 4.2 TiO₂ solution contact angle

4.1.3.1 Determination of The Contact Angle of Polymer Sample

In this research, the contact angle of groups, such as PVA and PMMA, were estimated by double sided contact angle estimation, as we did for metal oxide group sample.

For PVA, the contact angle estimation from right side was 29.52° and from left side was 27.60°. Optimization contact angle result for PVA was 28.56°. It has a high wetting capacity and has an appropriate contact angle for coating (Figure 4.3).

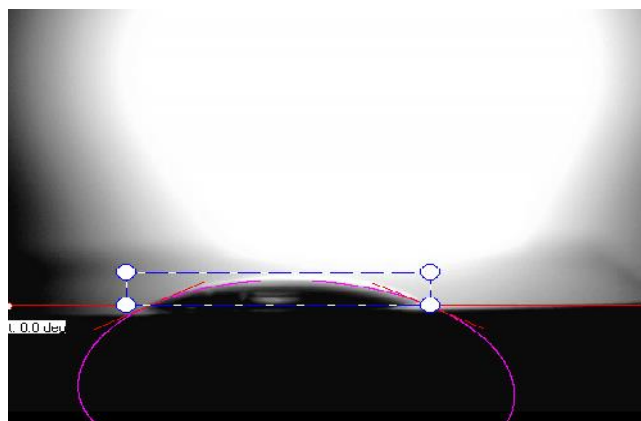


Figure 4.3 PVA solution contact angle

While estimated left contact angle for PMMA was 10.57° , the right was 18.38° . Average contact angle was 14.56° . Because the contact angle was below 90° , it has great wetting capacity, that is to say it is appropriate for coating (Figure 4.4).

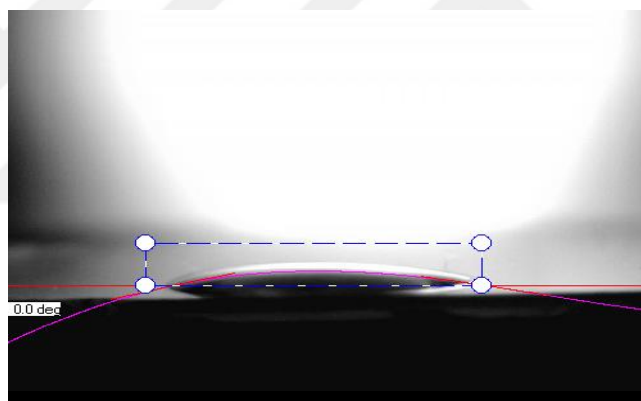


Figure 4.4 PMMA solution contact angle

4.2 Materials Process Optimization

4.2.1 Differential Thermal Analysis-Thermal Gravimetric Analysis (DTA-TGA)

Thermal analysis experiments were suitable for metal oxide group, polymer group. The heating regime for polymer group was; for PVA, 120 minutes, 75°C . As for PMMA, 130 minutes, 50°C dehydration was conducted. Because a high heating treatment for polymer group, as we did for metal oxides, is not possible.

By conducting DTA-TG study for metal oxides, heating treatment regime was identified. Hence, for Al_2O_3 and TiO_2 , two different DTA-TG process was applied (Figure 4.5 and Figure 4.6).

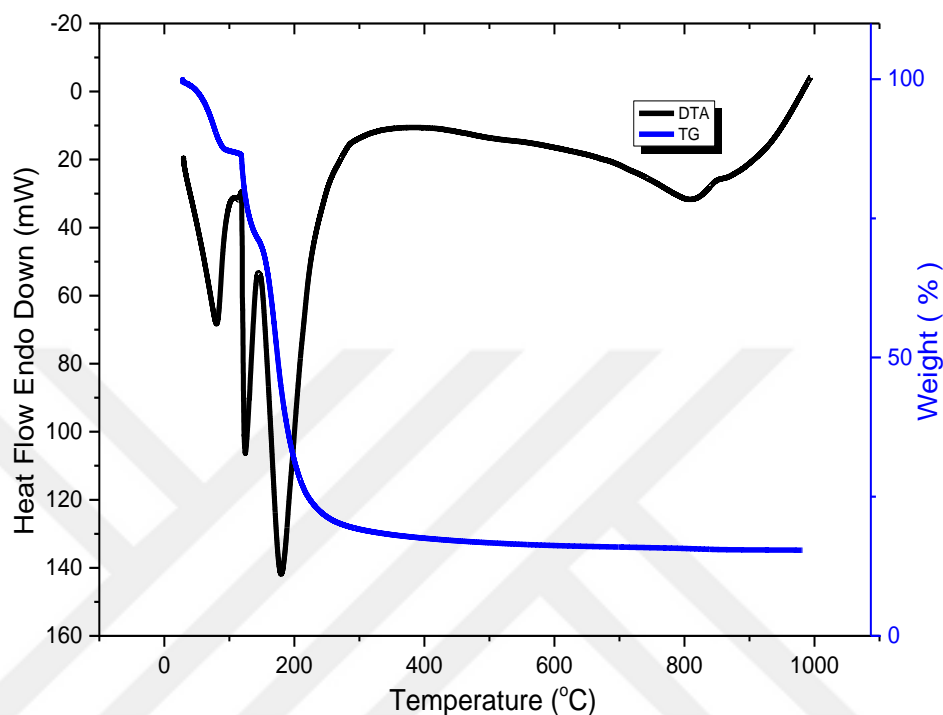


Figure 4.5 DTA-TG result for Al_2O_3 precursor solution

In the DTA-TG graphic given for Al_2O_3 analysis, certain changes were observed for certain temperatures. In order to comment on those changes, the study made by ROGOJAN et al., (2011) was used as a guide and heating treatment regime was determined as Al_2O_3 .

The first three endothermic effects of greater magnitude can be attributed to moisture water loss (the effect approximately 100-110 °C) and another endothermic effect is that hydroxyl loss from the decomposition of hydrated aluminium chloride and aluminium hydroxide, which can be possibly formed (the effects at 153 °C and 210 °C, respectively) it means that organic component decomposition. Final endothermic effect is at about 800 °C and 890 °C (Fig. 4.5) may be attributed to the transformation of polymorphous enantiotropy $\gamma\text{-Al}_2\text{O}_3$ in $\alpha\text{-Al}_2\text{O}_3$. and crystallite size characteristic to the nanopowders.

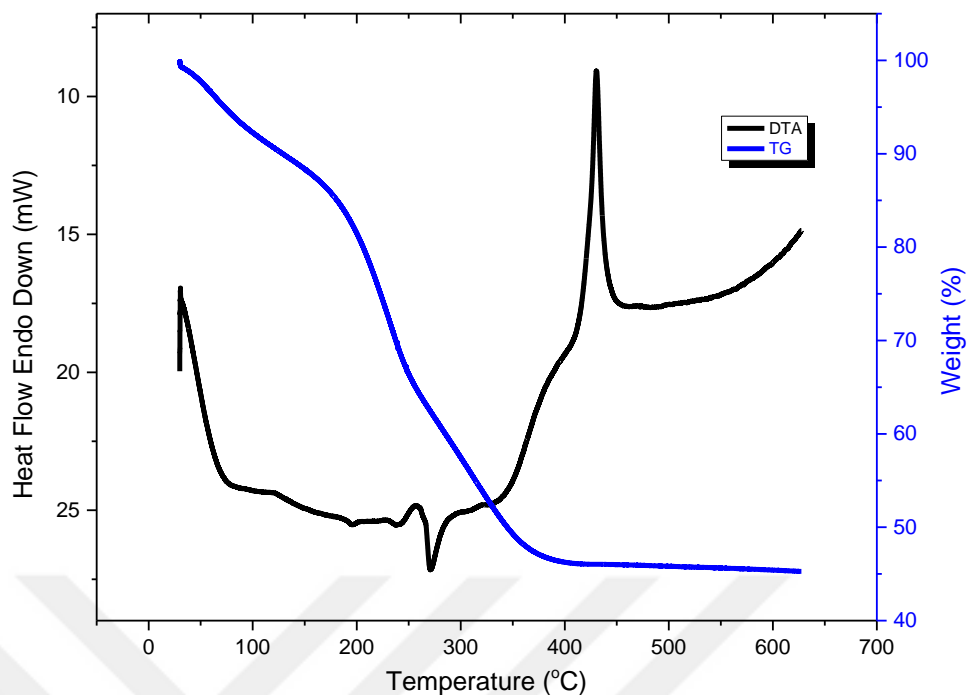


Figure 4.6 DTA-TG result for TiO₂ precursor solution

By DTA-TG analysis made for TiO₂, appropriate heating treatment regime was determined. The TiO₂ differential thermal analysis and thermal gravimetric analysis made under the supervision of the study of Foria et al., (2007) are: TiO₂ DTA-TG graphic showed rapid weight loss at around 100 °C resulting from the evaporation of residual solvent in the xerogel (powder), and another effect is that weight loss at around 270 °C: This effect due to decomposition of organic compounds such as acetic acid covalently bonded to TiO₂. The final result of TiO₂ graphic showed that the DTG curve of cyanidin-functionalized TiO₂ xerogel presented a peak at approximately 430 °C, which was not present in the DTG curve of TiO₂ xerogel and which can be attributed at cyanidin linked to TiO₂ decomposition. These results show us to the cyanidin transformed thermal stability form at approximately 420-430 °C.

4.2.2 Fourier Transform Infrared Spectroscopy (FTIR)

The aim of this section is to elucidate what type bonding can occur during heat treatment of metal oxide and polymeric materials, to understand the nature of their bonds, and thus to assist to be determined their process optimization.

In the context of this study, in order to observe change, samples from metal oxide group, such as Al_2O_3 and TiO_2 , were applied FT-IR treatment, one before, one after the heating treatment.

4.2.2.1 FT-IR Analysis for Metal Oxide Group

Firstly, in the context of this study, metal oxide group samples while they are in solution form and after calcination application, were FT-IR analysed two time.

Thus, chemical bounds occurred by heating treatment were observed. By those changes in chemical bounds and sol-gel method application, it was tried to observe whether sol-gel method coating is beneficial or not.

First of all, FT-IR analysis for Al_2O_3 in solution and after calcination were compared. Al_2O_3 in solution and calcined Al_2O_3 were given in Figure 4.7 and Figure 4.8.

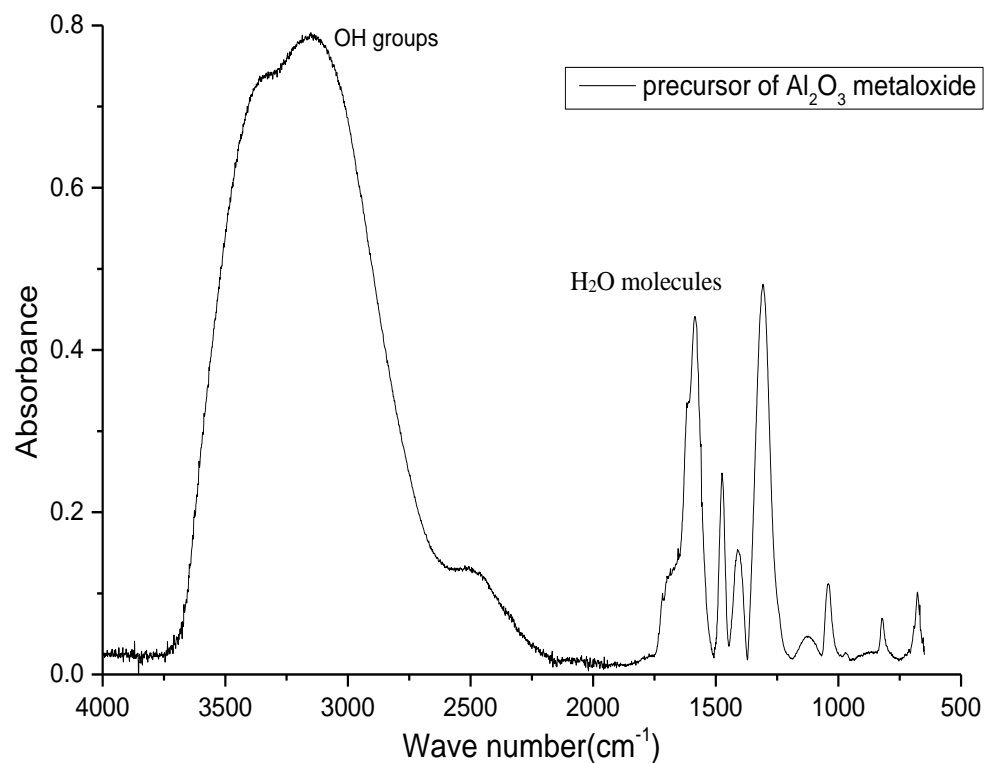


Figure 4.7 FT-IR result Al_2O_3 metal oxide precursor

Peaks can be seen approximately at 3000 cm^{-1} , 1800 cm^{-1} and 1300 cm^{-1} in first solution results for Al_2O_3 . After calcined with in this peaks were disappeared. So organic groups were disappeared by in this calcined processing. If we help us that peaks from Adamczyk & Długon (2011)' s research and explain; in this measurement, the bands assigned to the stretching vibrations of OH groups (at about $3200\text{--}3472\text{ cm}^{-1}$) together with the bending vibrations in H_2O molecules (at about $1350\text{--}1670\text{ cm}^{-1}$) are detected, what is connected with the sol-gel synthesis (Figure 4.7). Then these bands were disappeared due to calcined processing and confirming Al_2O_3 was obtained (Figure 4.8).

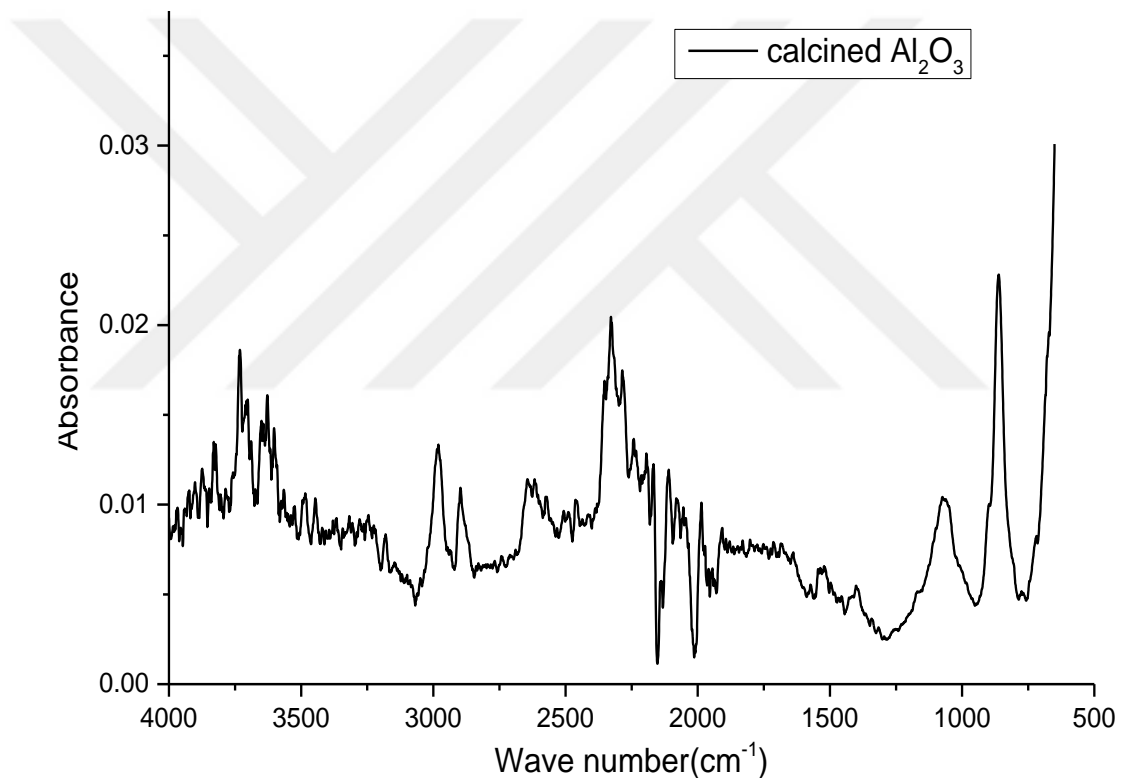


Figure 4.8 FT-IR result for calcined Al_2O_3

Afterwards, the metal oxide sample, which is TiO_2 sample, in solution form and in silicon coated on wafer form after heating treatment were FT-IR analysed. Here, the purpose is to observe any organic bound and determine whether there is the intended crystal structure.

In figures 4.9 and 4.10, FT-IR analysis of solution forms and calcined forms, in other words, coated forms can be seen.

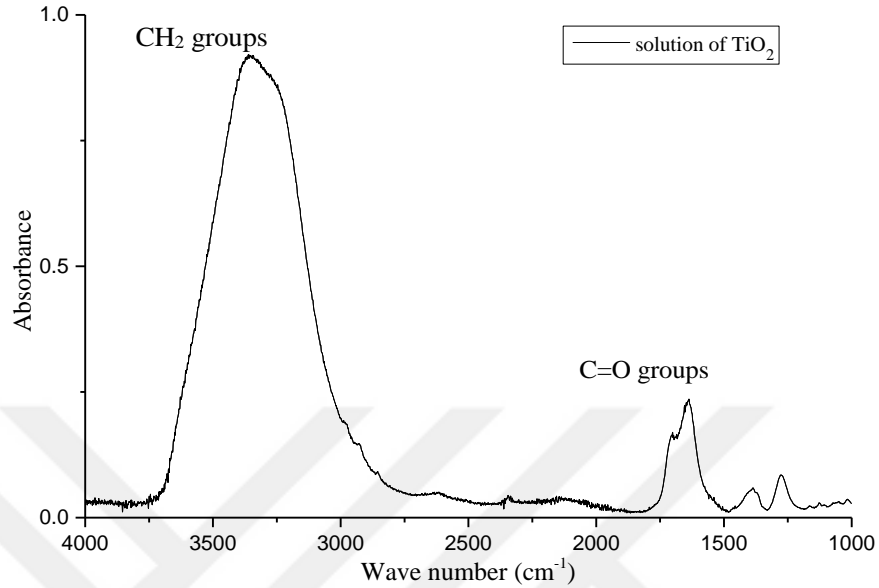


Figure 4.9 TiO₂ precursor metal oxide solution

ŞTEFAN et al., (2008) 's study helps that analysis for bands, so the strong vibration bands at about 2870 cm⁻¹ correlated with CH₂ groups, and vibrations in the 1600-1000 cm⁻¹ range, assigned to C=O groups, disappear in thermally treated samples (Figure 4.9).

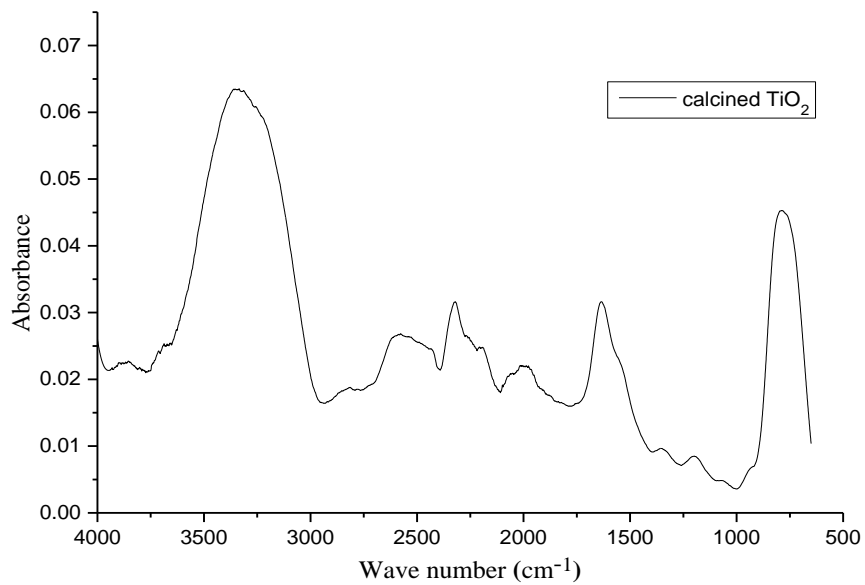


Figure 4.10 Calcined TiO₂

The thermal treatment leads to the partial or complete removal of ethanol and GAA. The porosity of these materials was evaluated by measuring the surface area of gel-sample containing bands (correlated CH₂ groups at about 3200-3400 cm⁻¹ and losing surface areas at about TiO₂ 700-800 cm⁻¹) after thermal treatment at 450°C. Finally, these FTIR analysis, thin film coatings are conforming for phase dielectric measurement (Figure 4.10).

4.2.2.1 FT-IR Analysis for Polymer Group

FT-IR analyses that belong to PVA and PMMA samples of polymer group were given in Figure 4.11 and 4.12.

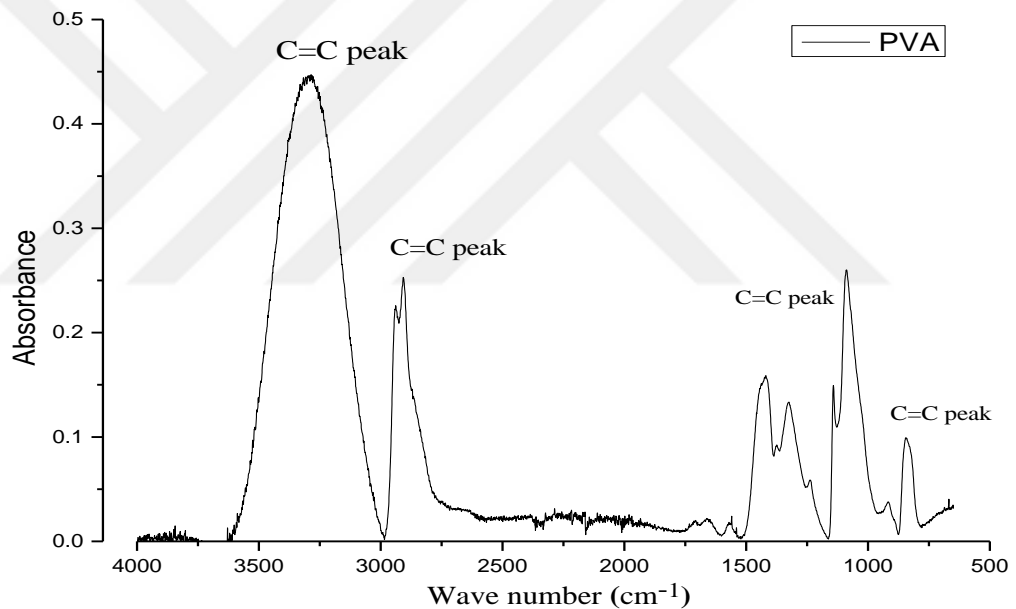


Figure 4.11 PVA FTIR analysis in air atmosphere

Thomas et al., (2007) researching leads to that graphic for PVA FTIR analysis. A large carbonyl peak around 1715 cm⁻¹ appears in the spectrum is observed to coincide with the first degradation step of the mass loss curves. This is indicative of the inclusion of atmospheric oxygen in the polymer. The carbonyl peak remains important in the degradation throughout the first degradation step and diminishes towards the end of this step. The second stage of the degradation a C=C peak appears about 3255, 2910, 1100 and 760 cm⁻¹ (Figure 4.11).

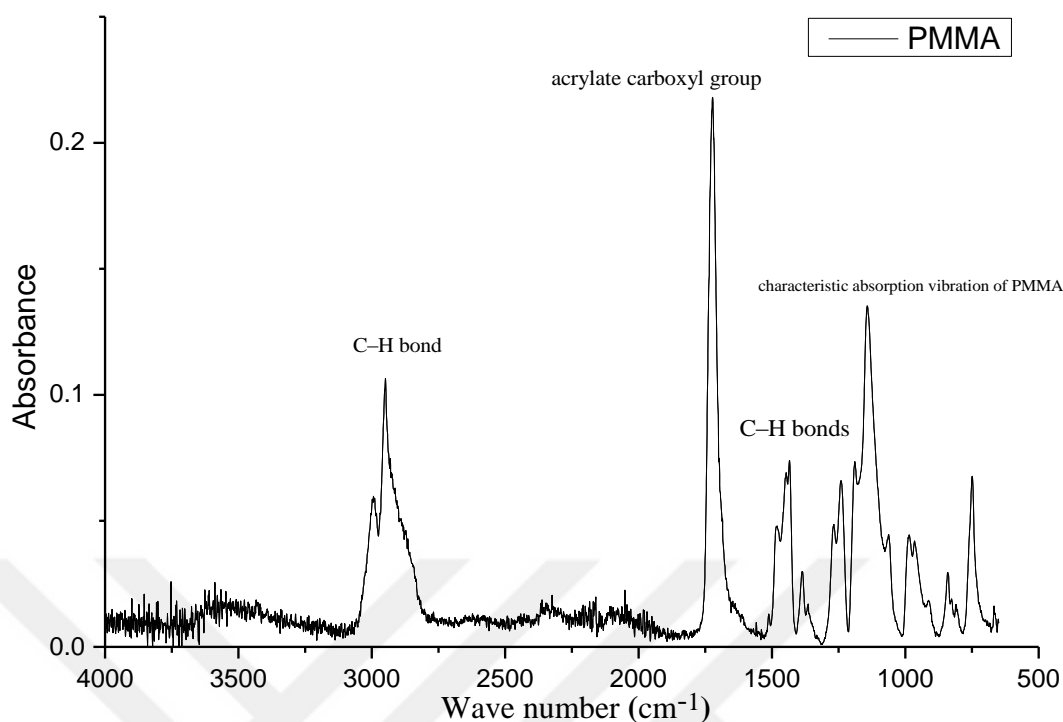


Figure 4.12 PMMA FTIR analysis in air atmosphere

Duan G. Et. al (2008) FTIR analysing for PMMA shows that the first band is 1400 cm^{-1} and 754 cm^{-1} can be attributed to the α -methyl group vibrations. The band at 1211 cm^{-1} is the characteristic absorption vibration of PMMA, together with the bands at 1062 cm^{-1} and 843 cm^{-1} . The band at 1725 cm^{-1} indicate the presence of the acrylate carboxyl group. The band at 1440 cm^{-1} can be attributed to the bending vibration of the C–H bonds of the $-\text{CH}_3$ group. The two bands at $2,997\text{ cm}^{-1}$ and $2,952\text{ cm}^{-1}$ can be assigned to the C–H bond stretching vibrations of the $-\text{CH}_3$ and $-\text{CH}_2-$ groups, respectively (Figure 4.12).

4.3 Phase Analysis

X-ray diffraction (XRD) patterns of thin films were determined by means of a Rigaku diffractometer with a Cu $K\alpha$ irradiation (wavelength, $\lambda=0.15418\text{ nm}$). Measurements were performed by applying voltage of 40 kV and current of 30 mA. Scans were made over the range $2\theta=0-90^\circ$ in increments of 2° .

4.3.1 Phase Analysis for Metal Oxide Samples

Figure 4.13 illustrate XRD pattern of Al_2O_3 film. As it can be seen in Figure 4.13 pure crystalline Al_2O_3 ceramic could be obtain by sol-gel spin coating method. There is no any different phase which is not Al_2O_3 . Likewise, TiO_2 film Al_2O_3 film on Si substrate does not include any impurity or unwanted structure. It is not possible to see any amorphous phase in Al_2O_3 thin film. Whole of it shows high crystallinity.

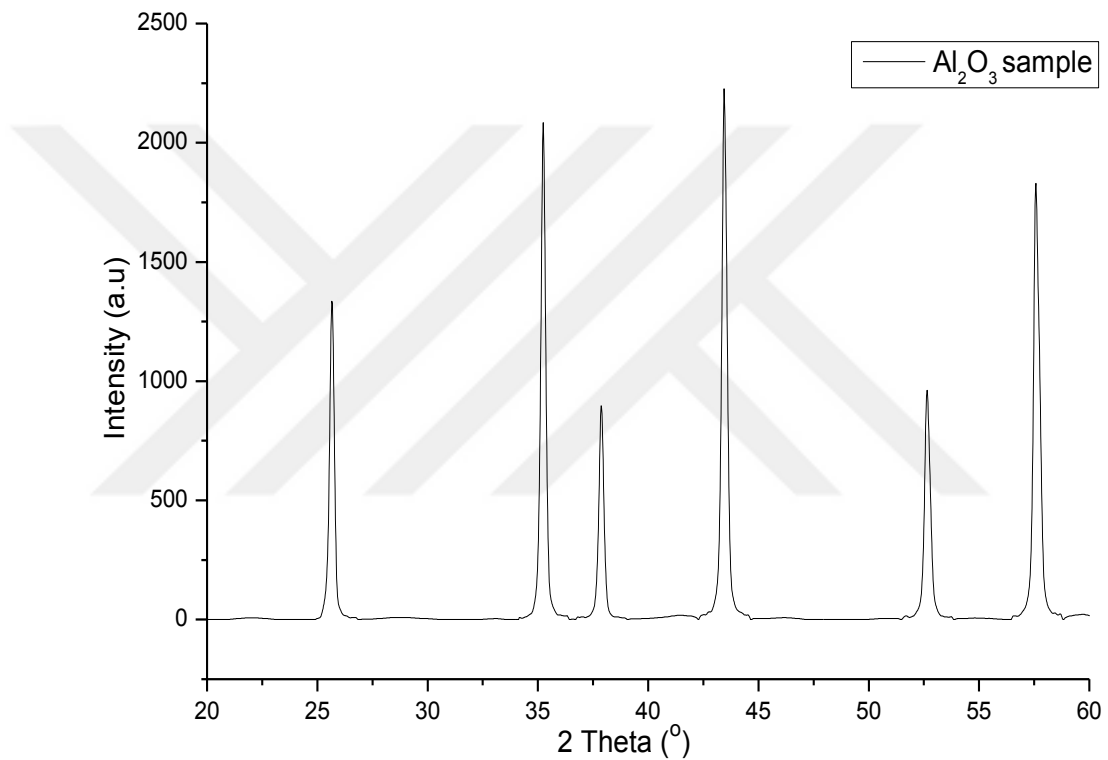


Figure 4.13 XRD pattern of Al_2O_3 thin film

Figure 4.14 illustrates XRD pattern of TiO_2 film. As it can be seen in Figure 4.14 pure crystalline anatase phase of TiO_2 ceramic could be obtain.

There is no any different phase which is not. In addition, the film has some rutile phase on it. It could be seen that the pattern of TiO_2 has some rutile peaks near the anatase peaks. The TiO_2 film on Si substrate doesn't include any impurity or unwanted structure. The film shows high crystallinity.

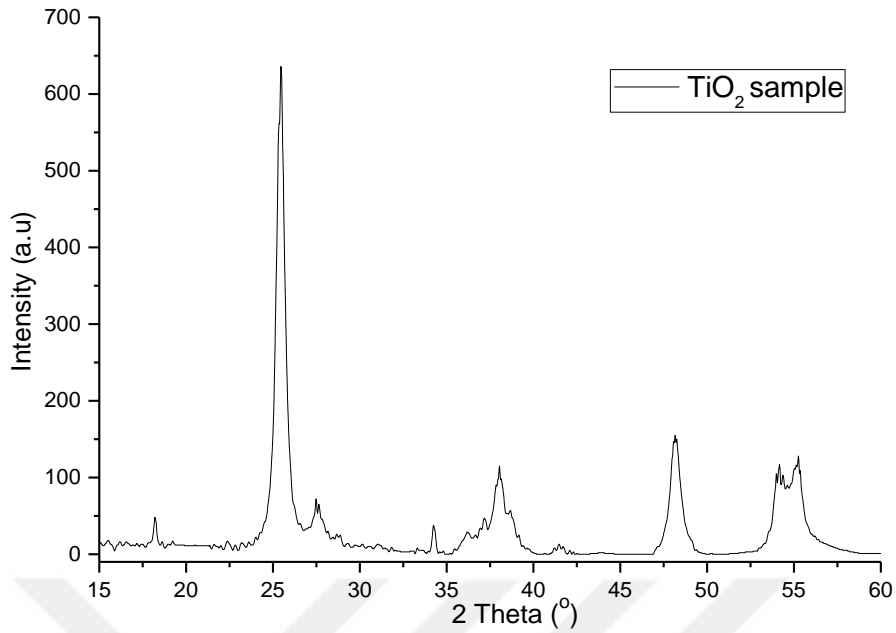


Figure 4.14 XRD pattern of TiO₂ thin film

4.3.2 Phase Analysis for Polymer Samples

Figure 4.15 depicts XRD pattern of spin coater derived PMMA film. The result is congruent with the FTIR spectrum which means that the PMMA film shows amorphous characteristic. It is obvious that The PMMA films doesn't include crystalline phase. Two peaks at 19° and 32° endorse the amorphousness of PMMA films.

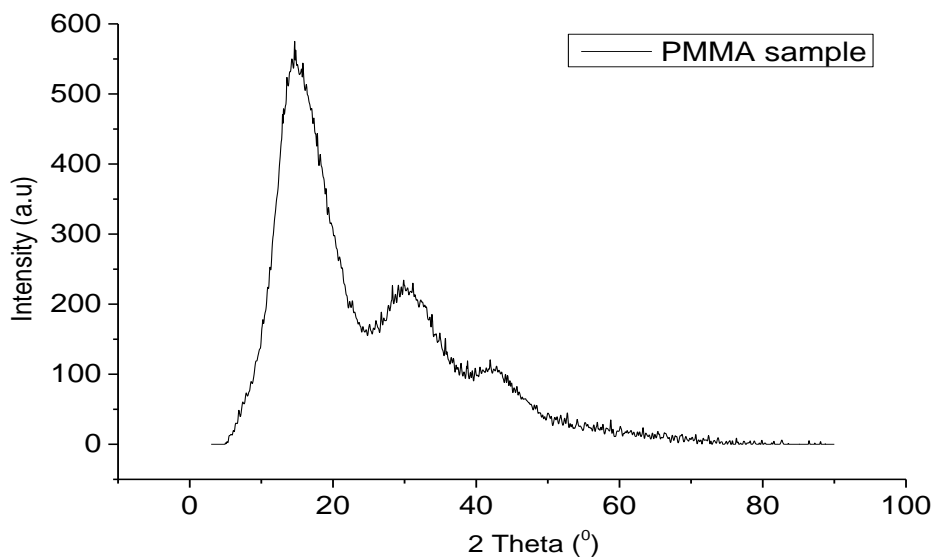


Figure 4.15 XRD pattern for PMMA thin film

The XRD pattern in Figure 4.16 illustrates an amorphous structure. This structure is resembling to PMMA, yet in Figure 4.16 which shows XRD pattern of PVA film on Si substrate only one peaks could be seen on spectra.

This suggests that PVA is more crystalline than PMMA. But it doesn't mean that PVA is a crystalline material. It still shows amorphous characteristic.

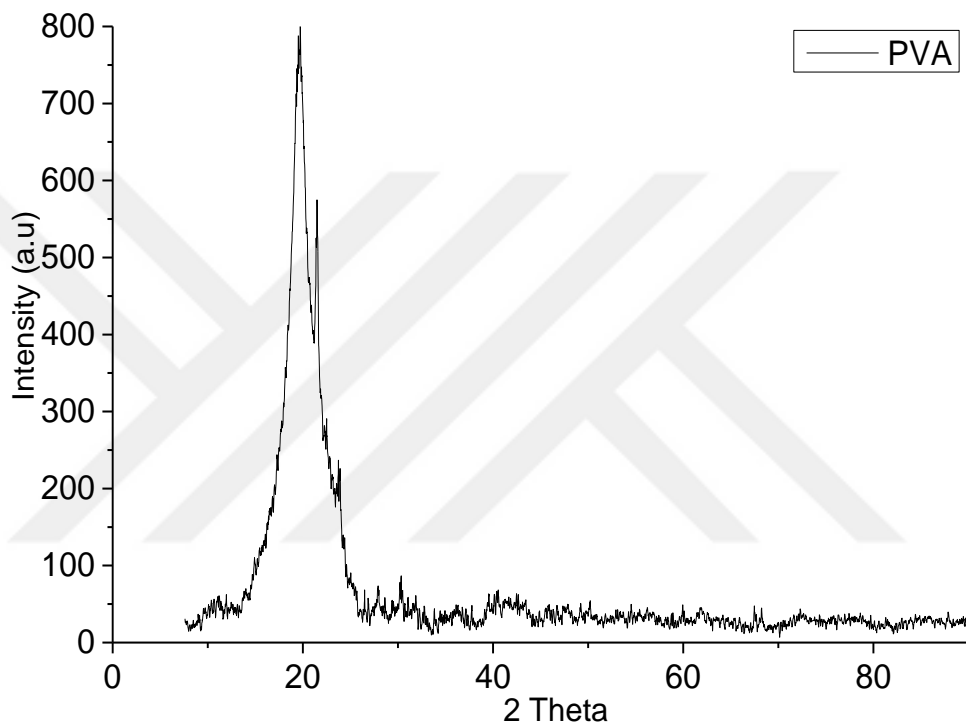


Figure 4.16 XRD result for PVA thin film

4.4 Microstructure Analysis / Energy Dispersive X-ray Spectroscopy (EDS)

The surface topographies and characteristics of films on Si substrates were examined by using SEM. Vacancies, micro cracks and porosities were examined by SEM for determining the grain size on the morphology of the thin films.

Additionally, elemental analysis of Al_2O_3 and TiO_2 coatings on Si substrates was investigated through EDS (Figures 4.17 and 4.18).

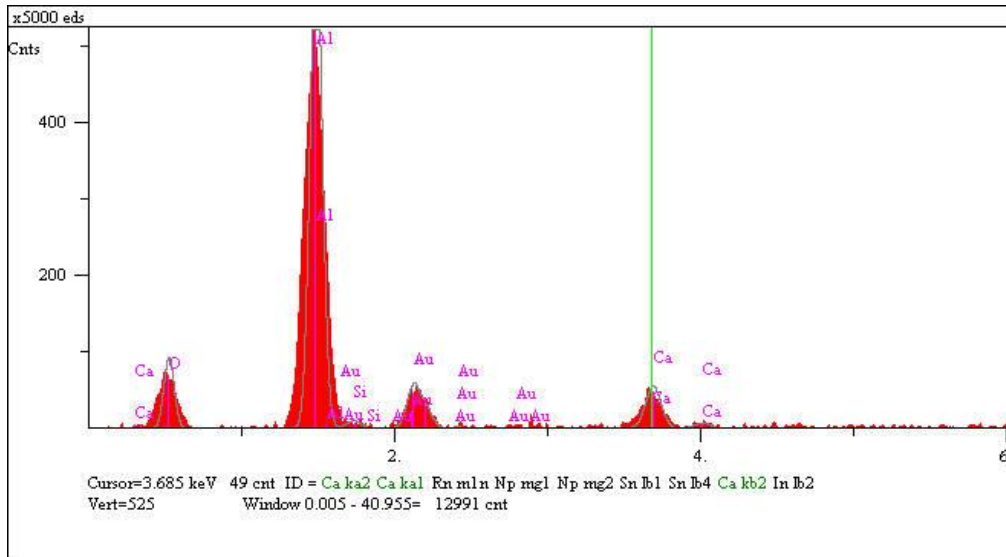


Figure 4.17 EDS result for Al₂O₃ thin film

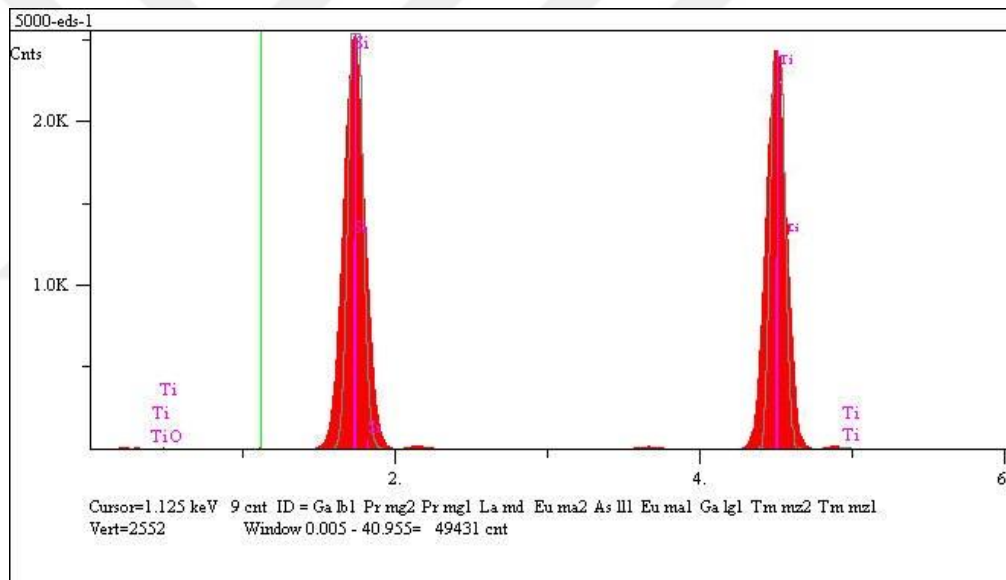


Figure 4.18 EDS result for TiO₂ thin film

4.4.1 Microstructure Properties of Metal Oxide Groups

Microstructures of the TiO₂ and Al₂O₃ films are given in figures between Figures 4.19 and 4.20 in detail. The TiO₂ films annealed at 500 °C. The Figures show that it is possible to obtain TiO₂ films having continuous and homogeneous microstructure by spin coating method and annealing at 500 °C for 1 hour in air. In Figure 4.19 (left side-a) depicted 1000x (magnitude) of TiO₂ film and Figure 4.19 (right side) depicted

5000x (magnitude) of TiO_2 film. SEM micrographs in Figure 4.19 showed that the films were crack-free structure on Si substrates.

The samples heat-treatment at 500°C yielded a homogeneous and smooth film surface. There are some particles like structure on film surface but they don't have significant effect on the film structure. The film is still proper to use in neurostimulator devices as dielectric layer.

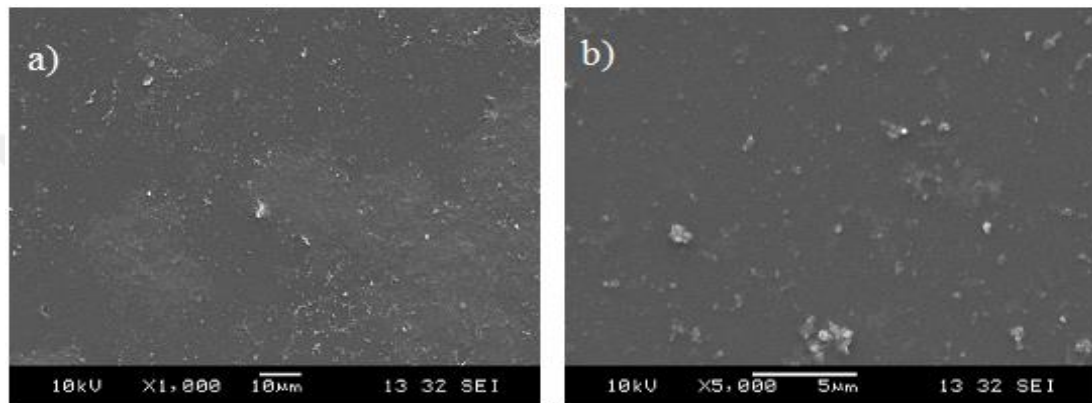


Figure 4.19 SEM result with depicted 1000x (a) and depicted 5000x (b) for TiO_2

Microstructures of the Al_2O_3 and films are given in figures between Figure 4.20 in detail. The Al_2O_3 films annealed at 1000°C . Figure 4.20 (left side) depicted 1000x (magnitude) of Al_2O_3 film and Figure 4.20 (right side) depicted 5000x (magnitude) of Al_2O_3 film.

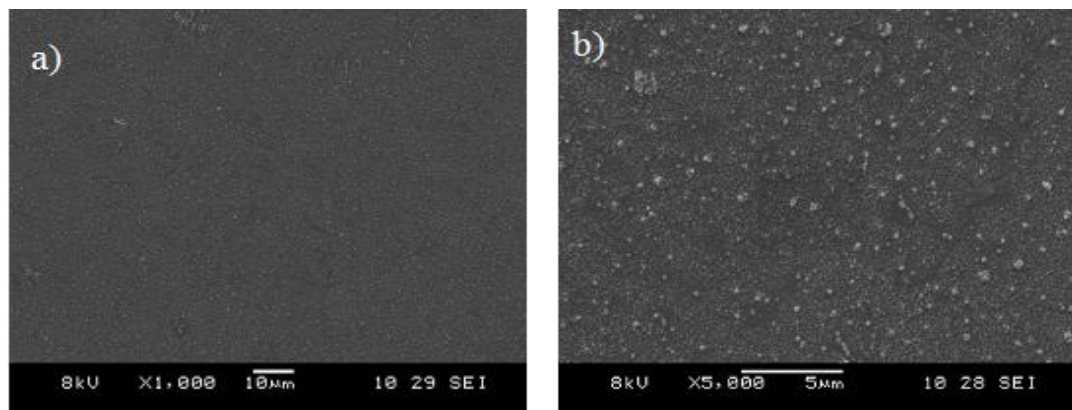


Figure 4.20 SEM result with depicted 1000x (a) and depicted 5000x (b) for Al_2O_3

As it can be seen the Al₂O₃ film doesn't include any pin hole and crack. This mean that like TiO₂ films Al₂O₃ film can be produce by spin coating then annealing at 1000 °C in air. The film has smooth and homogenous surface as well as TiO₂ film has. However, the particles like structure are available in Al₂O₃ film too. But as it was mentioned previously they don't effect negatively to film duty.

4.4.2 Microstructure Properties of Polymer Groups

Figure 4.21 shows polymeric thin film which is PVA and PMMA at different magnification, 500x and 5000x respectively. The films are very smooth and continuous. There is no crack or any nonhomogeneous structure.

This result proved the possibility of producibility of PVA and PMMA by cost effective spin coating method.

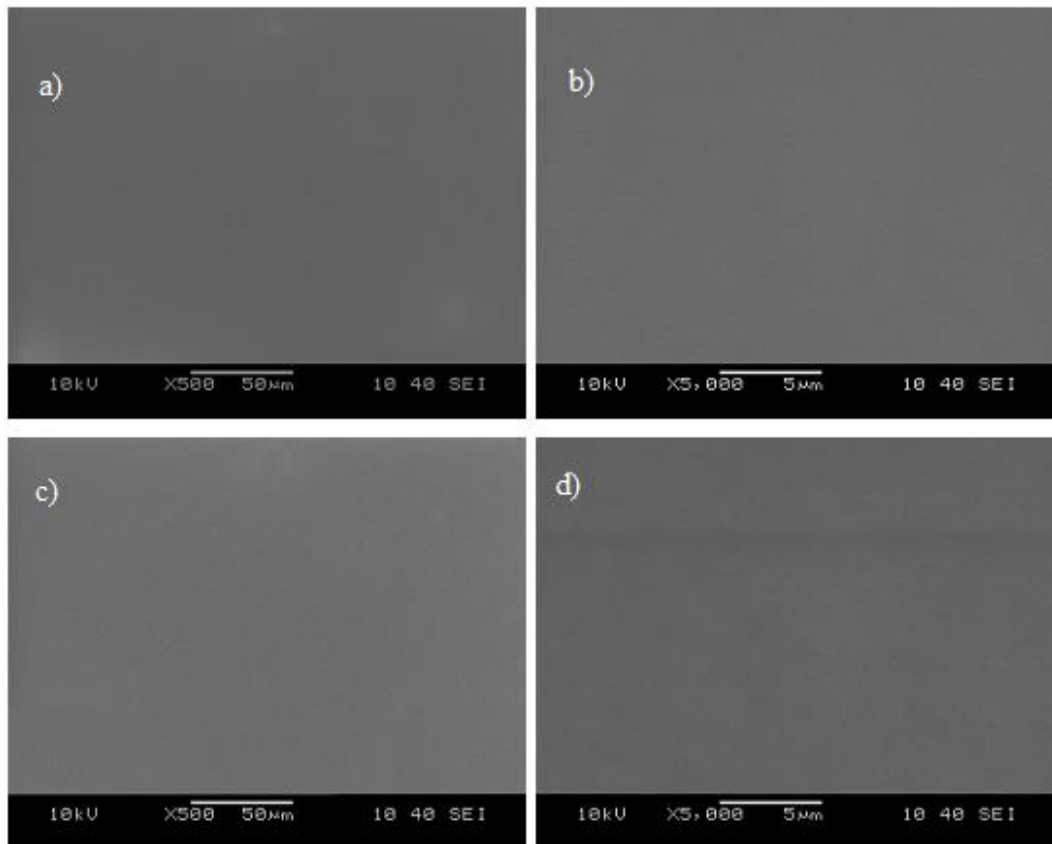


Figure 4.21 Polymeric thin film SEM results: a) PVA 500x, b) PVA 5000x; c) PMMA 500x, d) PMMA 5000x

4.5 Dielectric Properties

4.5.1 Dielectric Properties of Metal Oxide Groups

Variation of permittivity or dielectric constant (ϵ) as a function of frequency for Al_2O_3 at room temperature is as shown in Figure 4.22. Frequency range was determined 1Hz-1 MHz. Furthermore, it is observed that the charge carriers undergo dipole polarization at particular low frequency region of 10 Hz. Further, the increase in frequency decreases of the permittivity (ϵ) due to the electrical relaxation processes. In both high frequencies as well as at very low frequencies, there is a significant change permittivity.

The permittivity value of Al_2O_3 film is variable the range of 5 to 9.5. This is due to the dipolar contribution of charge carriers between one isolated to others states (Figure 4.22).

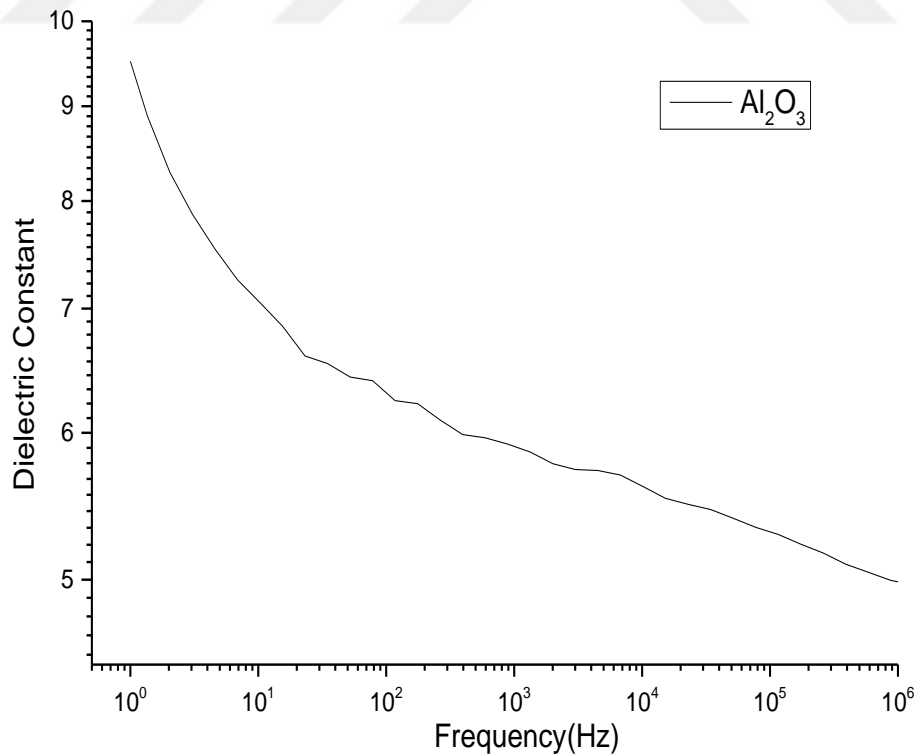


Figure 4.22 Permittivity of Al_2O_3 thin film

Figure 4.23 illustrate TiO_2 's dielectric constant versus frequency. For TiO_2 the increase in frequency decreases of the permittivity (ϵ) due to the electrical relaxation processes as well as Al_2O_3 . However dielectric constant of TiO_2 significantly higher than Al_2O_3 .

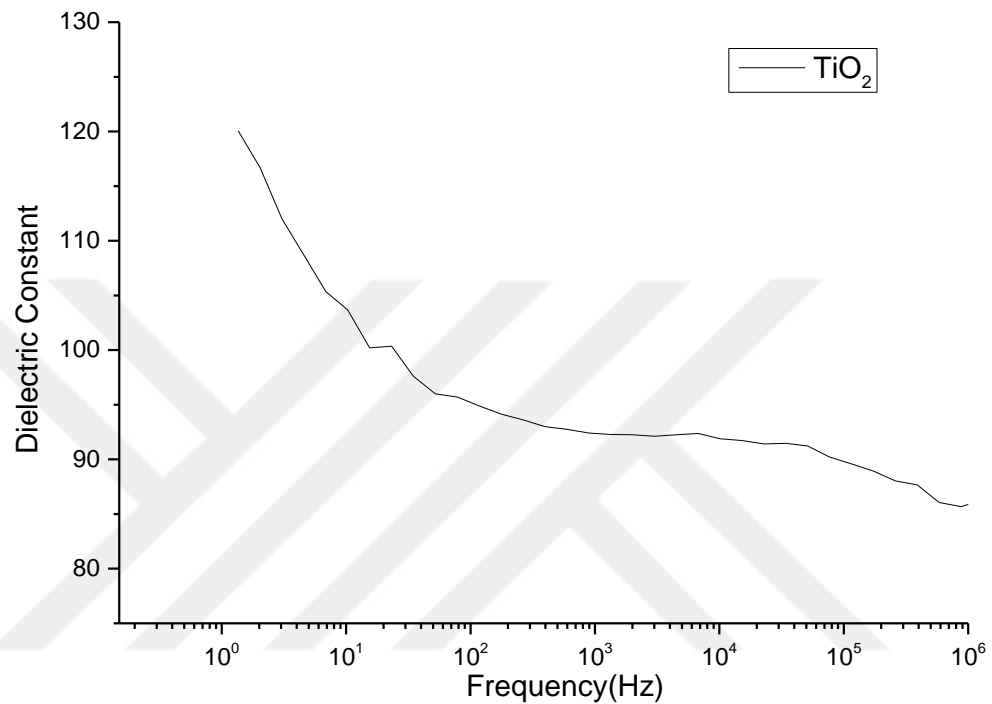


Figure 4.23 Permittivity of TiO_2 thin film

Furthermore, it is observed that the charge carriers undergo dipole polarization at particular low frequency region of 100 Hz. Dielectric Constant of TiO_2 is changeable range between 85 and 120. This indicates that dielectric loss of TiO_2 is higher than Al_2O_3 .

4.5.2 Dielectric Properties of Polymer Groups

Dielectric behaviour of PVA thin film is depicted in Figure 4.24. It is obvious that dielectric constant of polymeric PVA film is lower than metal oxide film which is 120 for TiO_2 and 9 for Al_2O_3 . As well as TiO_2 and Al_2O_3 , dielectric constant of PVA film increases with decreasing frequency. However, there is no apparent point of frequency which permittivity increases significantly.

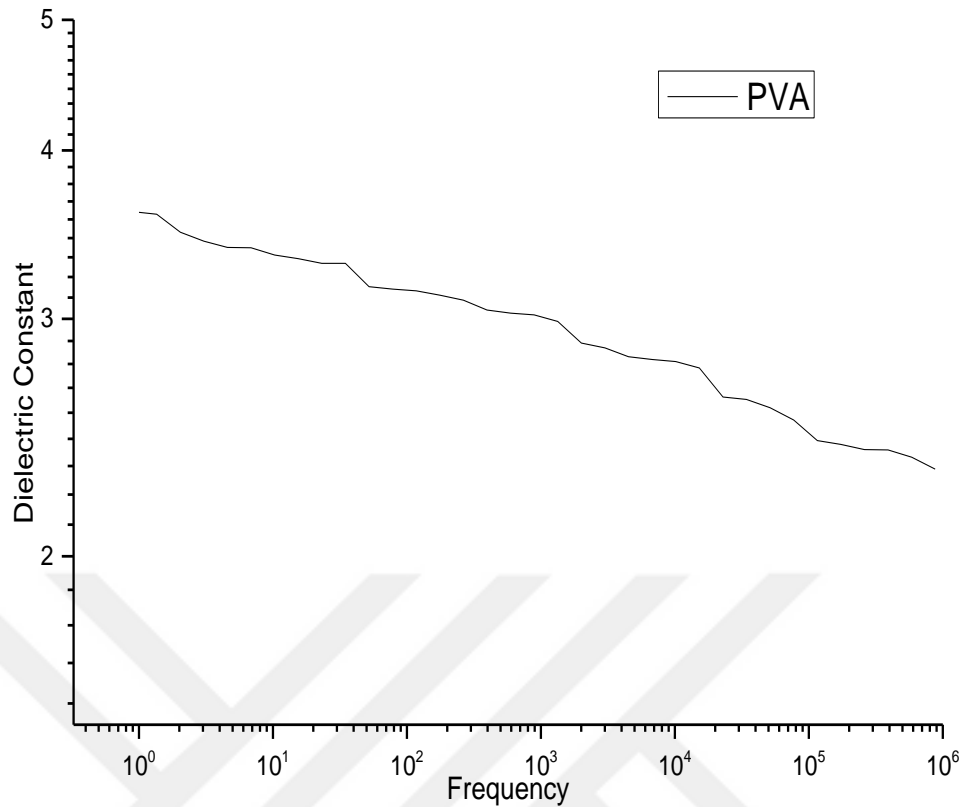


Figure 4.24 Permittivity of PVA

This means that PVA shows more stable dielectric behaviour. Whereas the dielectric constant of PVA is 2,2. At high frequency which is 10^6 , it is almost 4 for 1 Hz. The difference of the permittivity value between 10^6 Hz and 1 Hz is nearly 2.

The permittivity of PMMA versus frequency is very similar with PVA Figure 4.25. This is because of common polymer characteristic. In general, the dielectric constant of Polymeric material is not higher than 4-5. We can see same situation in our both PVA and PMMA results. Whereas the dielectric constant of PMMA is 2,5 at high frequency which is 10^6 , it is 3,5 for 1 Hz.

The difference of the permittivity value between 10^6 Hz and 1 Hz is nearly 1. We conclude that PMMA most stable dielectric material in our four different samples which are PVA, Al_2O_3 and TiO_2 .

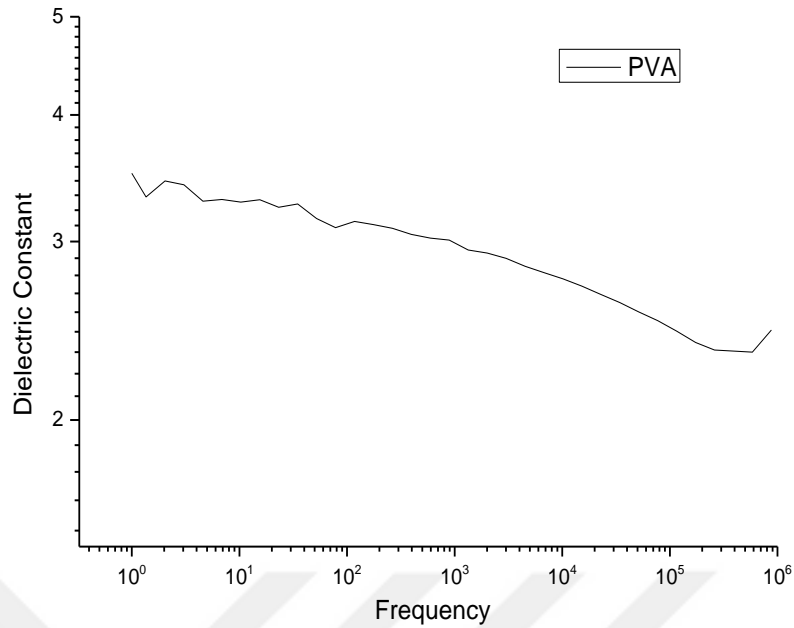


Figure 4.25 Permittivity of PMMA

According to these results, it would be inferred that TiO₂ has highest permittivity however this material shows high dielectric loss. Due to this phenomenon it is hard to applied TiO₂ in integrated circuit. On the other hand, lowest dielectric constant and loss is belonging to PMMA. We have different difficulties when use these two type materials. For instance, PMMA degrade at lower temperature while TiO₂ is more stable at high temperature.

And the result of dielectric measurement, we can use these materials on neurostimulator system. Because these dielectric result is suitable for human body and also this system can transmit on to another nerve from nerve.

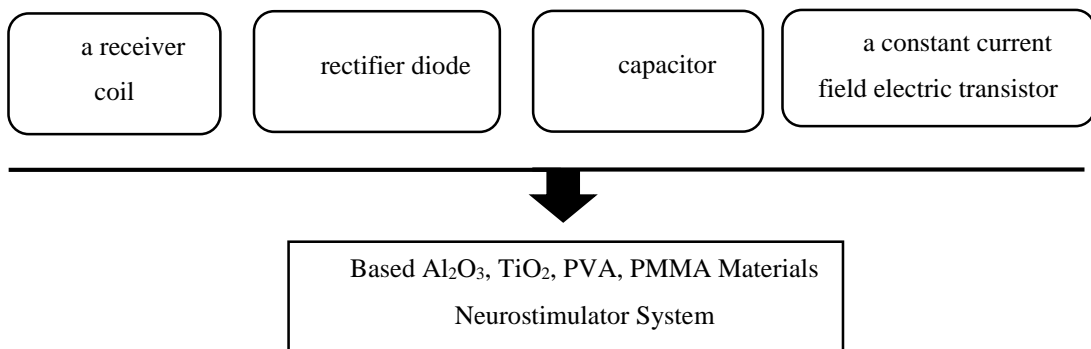


Figure 4.26 Design of neurostimulator system

CHAPTER FIVE

CONCLUSION AND FUTURE PLANS

5.1 General Results

In the context of this thesis, anatomical parts creating central or environmental (peripheral) nerve system, which are called neurostimulator were used. By placing electrodes in, on the surface or around those neurostimulators and with an applied special electrical tension, it was aimed to produce semi-conductive materials with sol-gel method and spin coating technique in order to produce related device that maintain activation and inhibition. Accordingly, it was observed that, in order to activate and inhibit the applied tension, the performance of electrical tension is specified by the performance of used semi-conductive material. The most significant factor that affect the electrical performance is dielectric constant. Thanks to the dielectric capacity of produced materials, current-volt balance can be maintained and modulation process can be conducted.

1. As a result of this study, literature researches of metal-oxide group belongings, Al_2O_3 and TiO_2 , were made and it was specified that they are being used for neurostimulator production. Hence, they were preferred. In the context of achieved results, dielectric capacity of Al_2O_3 was 9.5 and of TiO_2 was 120.
2. The other case study was constituted from polymer group, PVA and PMMA. Dielectric capacities of PVA and PMMA were 2.2 and 2.5. As a result, according to usage area and intended performance, different material choices can be made.
3. In order to specify dielectric features, the optimization result of materials and characterization were estimated. Within this framework, FT-IR, XRD, SEM, pH and turbidity estimations were made and it was observed whether there was a proper environment for electrical circuit design.
4. As it can be seen from the obtained results, by using sol-gel method, material diversity can be maintained which we can constitute a basis for neurostimulator with different performances.

5.2 Future Plans

By using sol gel and spin coating to produce coating on semi conductive silicon wafer, successful materials for neurostimulator production were maintained. Thanks to this study, by sol gel, it was seen that more efficient semi conductive materials with higher performances in dielectric features can be produced.

Within increasing technology, electrical based devices are in need of getting smaller. Sol gel constitutes a significant place among nanotechnological processes since both smaller and technological devices are needed. Efficiencies of Al_2O_3 , TiO_2 , PVA and PMMA can be seen in this study, if neurostimulator is to be produced. With different coating thickness and heating treatment, advanced electrical featured substructure elements can be produced.

At the same time, studies can be made in nanotechnology area. Thanks to the produced coating, electronic circuit design can be made, and by reproducing whole circuit elements, electrodes, antennas with nanotechnology, micro-sized neurostimulators may be even invisible with eye, can become possible.

In addition, in the field of medicine, neurostimulator kind of devices can be used for plucked and crushed nerves' treatment. Signals can be re-powered and transmitted successfully by producing similar based material production.

There is no doubt that in the future, neurostimulation will be used in different fields.

REFERENCES

- Adamczyk, A. & Długon, E., (2012). The FTIR studies of gels and thin films of Al₂O₃-TiO₂ and Al₂O₃-TiO₂-SiO₂ systems. *Spectrochimica Acta Part A: Molecular and Biomolecular Spectroscopy*, 89, 11-7.
- Addamo, M., Bellardita, M., Carriazo, D., Paola, A.D., Milioto, S., Palmisano, L. & Rives, V., (2008). Inorganic gels as precursors of TiO₂ photocatalysts prepared by low temperature microwave or thermal treatment. *Applied Catalysis B: Environmental*, 84, 742-748.
- Aegerter, A.M. & Mennig, M., (2004). *Sol-gel technologies for glass producers and users*. New York: Springer Science + Business Media.
- Aurobind, S.V., Amirthalingam, K.P. & Gomathi, H., (2006). Sol-gel based surface modification of electrodes for electro analysis. *Advances in Colloid and Interface Science*, 121, 1-7.
- Bayrakçeken, A., (2008). Platinum and platinum-ruthenium based catalysts on various Carbon supports prepared by different methods for pem fuel cell applications. *In Partial Fulfilment of the Requirements for the Degree of Doctor of Philosophy in Chemical Engineering*.
- Brinker, J.C. & Scherer, W.G., (1990). *Sol gel science: the physics and the chemistry of sol gel processing*. United State of America: Academic Press, Inc.
- Clapsaddle, B.J., Sprehn, D.W., Gash, A.E., Satcher, Jr.J.H. & Simpson, R.L., (2004). A versatile sol- gel synthesis route to metal-silicon mixed oxide nanocomposites that contain metal oxides as the major phase. *Journal of Non-Crystalline Solids*, 350, 173-181.

- Dilsiz, N. & Akovalı, G., (2002). Study of sol–gel processing for fabrication of low density alumina microspheres. *Materials Science and Engineering A*, 332, 91–96.
- Duan, G., Zhang, C., Li, A., Yang, X., Lu, L. & Wang, X., (2008). Preparation and characterization of mesoporous zirconia made by using a poly (methyl methacrylate) template. *Nanoscale Research Letters*, 3, 3, 118–122.
- Ebelioglu, F.M., (2009). *Processing, characterization and development of rare earth doped lead magnesium niobate ferroelectric ceramic capacitors by sol-gel technique*. PhD. Thesis, Dokuz Eylül University, İzmir.
- Erdogan, M., (1997). *Malzeme bilimi ve mühendislik malzemeler*. Ankara: Nobel Yayinevi.
- Faria, E. H., Marçal, L.A., Nassar J.E., Ciuffi, J.K. & Calefi, S.P., (2007). Sol-gel TiO₂ thin films sensitized with the mulberry pigment cyaniding. *Materials Research*, 10, 4, 413-417.
- Goldstein, J., Dale E. N, Patrick E., David C. J., Alton D. Romig Jr. Charles E. L., Charles F et. al., (1992). *Scanning electron microscopy and x-ray microanalysis*. New York: Springer Science + Business Media.
- Gover, K., (1996). *Measurement of microwave dielectric constants of some industrial materials*. M.Sc, Thesis Uludağ University, Bursa.
- Guglielmi, M. (1997). Sol-gel coatings on metals. *Journal of Sol-Gel Science and Technology*, 8, 443–449.
- Hamadani, M., Reisi-Vanani, A. & Majedi, A., (2010). Sol-gel preparation and characterization of Co/TiO₂ nanoparticles: application to the degradation of methyl orange. *Journal of the Iranian Chemical Society*, 7, 52-58.

- Hanaor, D., Trianni, G. & Sorrell, C. (2011). Morphology and photocatalytic activity of highly oriented mixed phase titanium dioxide thin film. *Surface and Coatings Technology*, 205, 12, 855-874.
- Hannan, A., Mutashar, S., Samad, A. & Hussain, A. (2014) Energy harvesting for the implantable biomedical devices: issues and challenge. *Biomedical Engineering OnLine*, 13, 79.
- Hellstrom, S.L. (2007). *Basic models of spin coating*. Stanford University: Course Work for Physics 210.
- Hill, J.O., (1991). *For better thermal analysis and calorimetry*. Canada: International Confederation for Thermal Analysis.
- Hirashima, H., Kojima, C., Kohama, K., Imai, H., Balek, V., Hamada, H. et al., (1998). Oxide aerogel catalysts. *Journal of Non-Crystalline Solids*, 225, 153–156.
- Innocenzi, P., Zub, Y.L.& Kessler, G.V. (2008). *Sol-gel methods for materials processing*. New York: Springer.
- Jones, R.W., (1989). *Fundamental principles of sol-gel technology*. London: The Institute of Metals.
- Jones, S.M., (1999). Gradient composition sol-gel materials. *Jet Propulsion Laboratory California Institute of Technology Pasadena*, 91, 109-8099.
- Kayatekin, I. (2006). *Synthesis and characterization of buffer layers and YBa₂Cu₃O_x superconducting coatings by chemical solution deposition method*. M.Sc. Thesis, Dokuz Eylül University, İzmir.

- Kazemi, M. & Mohammadizadeh, M.R. (2012). Simultaneous improvement of photocatalytic and superhydrophilicity properties of nano TiO₂ thin films. *Chemical Engineering Research and Design*, 90, 1473–1479.
- Keshmiri, M., Troczynski, T. & Mohseni M., (2006). Oxidation of gas phase trichloroethylene and toluene using composite sol–gel TiO₂ photocatalytic coatings. *Journal of Hazardous Materials B*, 128, 130–137.
- Li, W., Fries, D.P. & Malik, A., (2004). Sol–gel stationary phases for capillary electro chromatography. *Journal of Chromatography A*, 1044, 23–52.
- Livage, J., Beteille, F., Roux, C., Chatry, M. & Davidson P., (1998). Sol- gel synthesis of oxide materials. *Acta Materialia*, 46, 3, 743-750.
- Luis, A.M., Neves, M.C., Mendonca, M.H. & Monteiro, O., (2011). Influence of calcination parameters on the TiO₂ photocatalytic properties. *Materials Chemistry and Physics*, 125, 20–25.
- Mackenzie, J.D & Bescher, E.P., (2007). Chemical routes in the synthesis of nanomaterials using the sol–gel process. *Account of Chemical Research*, 40, 9, 810–818.
- Maruszewski, K., Streck, W., Jasiorski, M. & Ucyk, A., (2003). Technology and applications of sol-gel materials. *Radiation Effects & Defects in Solids*, 158, 439–450.
- Metroke, T.L., Parkhill, R.L. & Knobbe, E.T., (2001). Passivation of metal alloys using sol–gel derived materials — a review. *Progress in Organic Coatings*, 41, 233–238.
- Mitzi, D.B., Kosbar, L.L., Murray, C.E., Copel, M. & Atzali, A., (2004). High mobility ultrathin semiconducting films prepared by spin coating. *Nature*, 428, 299-303.

Niederberger, M. & Pinna, N., (2009). *Metal oxide nanoparticles in organic solvents*. New York: Heidelberg.

Olivo, J., Carrara, S., Member, IEEE, Michelli, D. G., Fellow, IEEE., (2011). Energy harvesting and remote powering for implantable biosensors. *IEEE Sensors Journal*, 11, 7.

Panescu, D., (2008). Implantable neurostimulation devices. *IEEE Engineering in Medicine and Biological Magazine*, 100-105.

Parpura, V., Silva, A.G., Tass, A.P., Bennet, E.K., Meyyappan, M., Koehne J. et al., (2013). Neuromodulation: Selected approaches and challenges. *Journal of Neurochemistry*, 124, 4, 436-53.

Peckham, P.H & Knutson, J.S., (2005). Functional electrical stimulation for neuromuscular application. *Annual Review Biomedical Engineering*, 7, 327-60.

Peeters, T. & Remoortere, B.V., (2008). Parameters of the spin coating process. *Journal and Applied Science*, 46, 685-696.

Pierre, A., C., (1998). *Introduction to sol-gel processing*. Publishers, Boston, Dordrecht. London: Kluwer Academic.

Porkodi, K. & Arokiamary, S., (2007). Synthesis and spectroscopic characterization of nanostructured anatase titania: a photocatalyst. *Materials Characterization*, 58, 495-503.

Rise, T.M., (2000). instrumentation for neuromodulation. *Archives of Medical Research*, 31, 237-247.

- Rogojan, R., Andronescu, E., Ghițulică, C. & Vasile, Ș.B., (2011). Synthesis and characterization of alumina nano-powder obtained by sol-gel method. *Scientific Bulletin-University Politehnica of Bucharest, Series B*, 73, 2.
- Ruys, J.A. & Mai, Y.W., (1999). The nanoparticle-coating process: a potential sol-gel route to homogeneous nanocomposites. *Materials Science and Engineering A*, 265, 202–207.
- Siouffi, A.M., (2003). Silica gel-based monoliths prepared by the sol–gel method: facts and figures. *Journal of Chromatography A*, 1000, 801–818.
- Ștefan, M., Popovici, J. E., Mureșan, L., Grecu, R. & Indrea, E., (2008). Preparation and characterisation of TiO₂ thin films with special optical properties. *Article in Journal of Optoelectronics and Advanced Materials*, 10, 9, 2228-2233.
- Thitinun, S., Thanabodeekij, N., Jamieson, A.M. & Wongkasemjit, S., (2003). Sol-gel processing of spiro-silicates. *Journal of the European Ceramic Society*, 23, 417–427.
- Thomas, S.P., Guerbois, P.J., Russell F.G. & Briscoe, B.J., (2001). *FT-IR* study of the thermal degradation of poly (vinyl alcohol). *Journal of Thermal Analysis and Calorimetry*, 64, 501-508.
- Tucker, C.A., Warwick, K. & Holderbaum, W., (2011). Efficient wireless power delivery for biomedical implants. *Institution Engineering and Technology Wireless Sensor Systems*, 2, 3, 173.
- Tyona, M.D., (2013). A theoretical study on spin coating technique. *Advances in Materials Research*, 2, 4, 195-208.

- Vasilyeva, M.A., Lounev, I.V. & Gusev, Y.A., (2013). *The methodology of the experiment on the dielectric spectrometer. Novocontrol BDS concept 80*. Study Guide The Kazan Federal University Institute of Physics.
- Wilde, F. D. & Gibs, J., (2002). *Turbidity: Geological survey*. In the United State of America: Techniques of Water-Resources Investigations.
- Ya-Yu, H., Kan-Sen, C., (2003). Studies on the spin coating process of silica films. *Ceramics International*, 29, 485–493.
- You, X., Chen, V. & Zhang, J., (2005). Effects of calcination on the physical and photocatalytic properties of TiO₂ powders prepared by sol–gel template method. *Journal of Sol-Gel Science and Technology*, 34, 181–187.
- Yuan, F., (2011). *CMOS circuits for passive wireless microsystems*. New York: Springer Science Business Media, LLC.
- Yuan, Y., & Lee, T. R., (2013). *Contact angle and wetting properties*. In Surface Science Techniques. Berlin; Heidelberg.
- Zabova, H., Sobek, J., Církva, V., Solcova, O., Kment, S. & Ha'jek, M., (2009). efficient preparation of nanocrystalline anatase TiO₂ and V/TiO₂ thin layers using microwave drying and/or microwave calcinations technique. *Journal of SolidState Chemistry*, 182, 3387–3392.
- Znaidi, L., (2010) Sol–gel deposited ZnO thin films: A review. *Materials Science and Engineering B*, 174, 18–30.